Computers and Mathematics with Applications 60 (2010) 541–562

Contents lists available at ScienceDirect

Computers and Mathematics with Applications

journal homepage: www.elsevier.com/locate/camwa

Modeling of decentralized linear observer and tracker for a class of unknown interconnected large-scale sampled-data nonlinear systems with closed-loop decoupling property

Jason Sheng-Hong Tsai [a,*], Nien-Tsu Hu [a], Po-Chuan Yang [a], Shu-Mei Guo [b], Leang-San Shieh [c]

[a] Department of Electrical Engineering, National Cheng Kung University, Tainan 701, Taiwan, ROC

[b] Department of Computer Science and Information Engineering, National Cheng Kung University, Tainan 701, Taiwan, ROC

[c] Department of Electrical and Computer Engineering, University of Houston, Houston, TX 77204-4005, USA

ARTICLE INFO

Article history:
Received 16 September 2009
Received in revised form 7 May 2010
Accepted 7 May 2010

Keywords:
Observer
Tracker
Large-scale system
Observer/Kalman filter identification
Digital redesign

ABSTRACT

A novel low-order modeling of decentralized linear observer-based tracker is presented in this paper for a class of unknown interconnected large-scale sampled-data nonlinear systems with closed-loop decoupling property. The appropriate (low-)order decentralized linear observer is determined by the off-line observer/Kalman filter identification (OKID) methodology and has been further improved based on the digital-redesign approach. Then the decentralized digital-redesign tracker with the high gain property is proposed, so that the closed-loop system has the decoupling property. The proposed approach is quite simple and effective for the complicate interconnected large-scale sampled-data system with known or unknown system.

1. Introduction

In recent years, the decentralized control of interconnected large-scale systems has been one of the popular research topics in control theory. Large-scale systems, such as transportation systems, power systems, communications systems, etc., are essential features of our modern life [1,2]. Many works on the subject have appeared in [3], and various methods have been used to deal with this problem. Among these methods, the well-known methodology is called decentralized adaptive control method, which was proposed by Ioannou [4] in 1986, and first showed that interconnections even though weak can make a decentralized adaptive controller unstable. From then on, a large amount of decentralized adaptive techniques have been developed in [5–17]. However, the methods [5–17] are based on the known system and known interconnections. When the system equation and interconnections cannot be obtained, the previous methods cannot be used any more. As a result, the proposed method for the unknown large-scale system is discussed later.

In this paper, low-order modeling of decentralized linear observer and tracker for a class of (unknown) interconnected large-scale sampled-data nonlinear systems with closed-loop decoupling property is proposed. First, the appropriate (low-)order decentralized linear observer for the sampled-data nonlinear system is determined by the off-line observer/Kalman filter identification (OKID) method [18]. The OKID method is a time-domain technique that identifies a discrete input–output mapping in the general coordinate form by using known input–output sampled data, through an extension of the eigensystem realization algorithm (ERA), so that the order-determination problem existing in the system identification problem can be solved. Then, each subsystem of the large-scale system is identified as a linear model.

* Corresponding author. Tel.: +886 6 2757575x62360; fax: +886 6 2345482.
E-mail address: shtsai@mail.ncku.edu.tw (J.S.-H. Tsai).

0898-1221/$ – see front matter © 2010 Elsevier Ltd. All rights reserved.
doi:10.1016/j.camwa.2010.05.002

Furthermore, the above observer has been improved based on the digital-redesign approach [19]. The digital-redesign approach is to pre-design an analog controller for the original analog plant and then carry out the digital redesign for the pre-designed analog controller without losing the high-performance tracking purpose. The observer-based digital-redesign tracker is a closed-loop controller with the state-feedback gain K_d and the feed-forward gain E_d used to control the plant to trace the desired trajectory. Sequentially, the decentralized digital-redesign tracker with the high-gain property is proposed, so that the closed-loop system has the decoupling property. And the proposed approach is quite simple and effective for the complicate large-scale sampled-data nonlinear system with known or unknown system equation.

There are many digital-redesign methods reported in literature; however, most digital-redesign techniques are implicitly retained the closed-loop stability and are based on the approximation techniques, in which the discrete system matrix of the original closed-loop analogue control system is approximately estimated and used to develop the digitally redesigned controller by state matching. Because the dimension of the input is generally less than state, the stability of the closed-loop system is not always assured [20]. One of those popular digital-redesign methods is the Tustin (bilinear) transformation. Based on Tustin's approach, the closed-loop stability may become unstable if sampling time is set too large. Recently, the reported results on the stability analysis of digital redesign such as [21–24] have been proposed so that the closed-loop controlled system is stable and longer sampling time is feasible by linear matrix inequality approach.

The rest of the paper is organized as follows. The problem description is given in Section 2. In Section 3, the observer/Kalman filter identification (OKID) method is introduced which is used to obtain the global behavior linear models of the subsystem in the interconnected large-scale system. Section 4 presents the improved observer-based digital-redesign tracker. And the design procedure is listed in Section 5. The simulations of linear/nonlinear systems are illustrated in Section 6 to demonstrate the methodology proposed in this paper.

2. Problem description

Consider the unknown nonlinear system consisting of N inter-connected MIMO subsystems shown as

$$\Sigma_i : \dot{x}_i(t) = f_i(x_i(t)) + g_i(x_i(t)) \left[u_i(t) + \sum_{j=1, j\neq i}^{N} h_{ij}(x_j(t - \tau_{ij})) \right], \tag{1a}$$

$$y_i(t) = C_i x_i(t), \tag{1b}$$

where $i = 1, 2, \ldots, N$, $u_i(t) \in \Re^{p_i}$ is the input, $y_i(t) \in \Re^{m_i}$ is the output and $x_i(t) \in \Re^{n_i}$ is the state vector to the ith subsystem at time t. $f_i(\cdot) \in \Re^{n_i \times n_i}$ and $g(\cdot) \in \Re^{n_i \times p_i}$ are nonlinear functions of the states $x_i(t)$ of Σ_i. The interconnected terms $h_{ij}(\cdot) : \Re^{n_i} \to \Re^{p_i} (j \neq i)$ between subsystems corresponding to the disturbances on the subsystem Σ_i due to subsystems Σ_j which represent the unknown nonlinear functions of the states $x_j(t)$, and τ_{ij} represent the time delays of the interconnections form Subsystem j to Subsystem i.

First, the appropriate (low-)order decentralized linear observer for the sampled-data nonlinear system is to be determined by the off-line observer/Kalman filter identification (OKID) method. Here, the OKID method can be applied to identify each subsystem as its linear model and the individual observer gain can also be obtained. Then, in order to overcome the effect of modeling error on the identified linear model of each subsystem, an improved observer with high gain property based on the digital-redesign approach will be developed to replace the identified observer by OKID. Sequentially, the decentralized digital-redesign tracker with the high gain property shown in Fig. 4 will be proposed, so that the closed-loop system has the decoupling property and well-tracking performance.

3. Observer/Kalman filter identification

In this section, the OKID formulation are derived to compute the system Markov parameters $Y_k = CG^{k-1}H$ and the observer gain Markov parameters $Y_k^0 = CG^{k-1}F$ form the observer Markov parameters $\overline{Y}_k = C\overline{G}^{k-1}\overline{H}$. Then, the combined system and observer gain Markov parameters Υ_k are used to construct a Hankel matrix. Finally, the constructed Hankel matrix is used to obtain the system and observer matrices $[G, H, C, F]$ by ERA.

3.1. Basic observer equation

The discrete-time state-space model of a multivariable linear system can be represented in the following general form:

$$x(k+1) = Gx(k) + Hu(k), \tag{2a}$$

$$y(k) = Cx(k), \tag{2b}$$

where $x(k) \in \Re^n$, $y(k) \in \Re^p$ and $u(k) \in \Re^m$ are state, output, and control input vectors, respectively, and $G \in \Re^{n\times n}$, $H \in \Re^{n\times m}$ and $C \in \Re^{p\times n}$ are system, input, and output system matrices, respectively. Assuming zero initial condition

$x(0) = 0$, system (2) for $k = 0, 1, 2, \ldots, l$ can be written explicitly as

$$\begin{aligned}
&x(0) = 0; \qquad y(0) = 0,\\
&x(1) = Hu(0); \qquad y(1) = CHu(0),\\
&x(2) = GHu(0) + Hu(1); \qquad y(2) = CGHu(0) + CHu(1),\\
&\vdots\\
&x(l) = \sum_{i=1}^{l} G^{i-1}Hu(l-i); \qquad y(l) = \sum_{i=1}^{l} CG^{i-1}Hu(l-i).
\end{aligned} \tag{3}$$

Eq. (3) can be grouped in a matrix form to yield

$$y = YU, \tag{4a}$$

where

$$y = [\, y(1) \quad y(2) \quad \cdots \quad y(l) \,], \tag{4b}$$

$$Y = [\, CH \quad CGH \quad \cdots \quad CG^{l-1}H \,], \tag{4c}$$

and

$$U = \begin{bmatrix} u(0) & u(1) & u(2) & \cdots & u(l-1) \\ 0 & u(0) & u(1) & \cdots & u(l-2) \\ 0 & 0 & u(0) & \cdots & u(l-3) \\ \vdots & \ddots & \ddots & \ddots & \vdots \\ 0 & 0 & 0 & \cdots & u(0) \end{bmatrix}, \tag{4d}$$

$y \in \Re^{p\times l}$, $Y \in \Re^{p\times ml}$, $U \in \Re^{ml\times l}$, p is the number of outputs, l is the number of data samples and m is the number of inputs. Eq. (4a) is a matrix representation of the relationship between the input and output time histories. Matrix Y contains all the Markov parameters $CH, CGH, \ldots, CG^{l-1}H$ to be determined. Matrix U is a block upper-triangular input matrix.

When the states of system are inaccessible, an observer is usually applied to estimate the states from the information of input and output. Therefore, add and subtract the term $Fy(k)$, the observer of system (2) can be rewritten as

$$\begin{aligned}
x(k+1) &= Gx(k) + Hu(k) + Fy(k) - Fy(k)\\
&= (G + FC)x(k) + Hu(k) - Fy(k)\\
&= \overline{G}x(k) + \overline{H}\overline{v}(k),
\end{aligned} \tag{5}$$

where $\overline{G} = G + FC$, $\overline{H} = [H, -F]$, $\overline{v}(k) = \begin{bmatrix} u(k) \\ y(k) \end{bmatrix}$, and F is an $n \times p$ arbitrary matrix that can be used to make the desired stable matrix $\overline{G}$. In fact, system (5) is an observer equation if the state $x(k)$ is considered as an observer state vector. Therefore, the Markov parameters of system (5) will be referred to as the observer Markov parameters. System (5) development can be interpreted by the viewpoint of [25], to place all the eigenvalues of $\overline{G}$ at the origin, i.e., a deadbeat observer. This provides that $C\overline{G}^k\overline{H} = 0$ for $k \geq q$. When using real data including noise, the eigenvalues of $\overline{G}$ are in fact placed such that $C\overline{G}^k\overline{H} \approx 0$ for $k \geq q$, where q is a sufficiently large integer. Note that $\overline{v}(k)$ is the input vector to the new observer-augmented system (5) and is composed of the nominal system (2) with inputs and outputs.

The above derivation is to be assumed zero initial conditions $x(0) = 0$. For nonzero initial conditions $x(0) \neq 0$, the following approach should be used. From system (5), it is easy to show that

$$\begin{aligned}
&x(k+1) = \overline{G}x(k) + \overline{H}\overline{v}(k),\\
&x(k+2) = \overline{G}x(k+1) + \overline{H}\overline{v}(k+1)\\
&\qquad = \overline{G}^2x(k) + \overline{G}\overline{H}\overline{v}(k) + \overline{H}\overline{v}(k+1),\\
&\vdots\\
&x(k+q) = \overline{G}x(k+q-1) + \overline{H}\overline{v}(k+q-1)\\
&\qquad = \overline{G}^q x(k) + \overline{G}^{q-1}\overline{H}\overline{v}(k) + \overline{G}^{q-2}\overline{H}\overline{v}(k+1) + \cdots + \overline{H}\overline{v}(k+q-1).
\end{aligned} \tag{6}$$

Then, the measurement equation (2b) can be rewritten as

$$\begin{aligned}
y(k+q) &= Cx(k+q)\\
&= C\overline{G}^q x(k) + C\overline{G}^{q-1}\overline{H}\overline{v}(k) + C\overline{G}^{q-2}\overline{H}\overline{v}(k+1) + \cdots + C\overline{H}\overline{v}(k+q-1).
\end{aligned} \tag{7}$$

Eq. (7) for $k = 0, \ldots, l-q$, can be written as

$$\overline{y} = C\overline{G}^{q}x + \overline{Y}\overline{V}, \tag{8a}$$

where

$$\overline{y} = [y(q) \quad y(q+1) \quad \cdots \quad y(l)] \in \Re^{m\times(l-q+1)}, \tag{8b}$$

$$x = [x(0) \quad x(1) \quad \cdots \quad x(l-q)] \in \Re^{l-q+1}, \tag{8c}$$

$$\overline{Y} = [C\overline{H} \quad C\overline{G}\overline{H} \quad \cdots \quad C\overline{G}^{(q-1)}\overline{H}] \in \Re^{m\times(p+m)q}, \tag{8d}$$

and

$$\overline{V} = \begin{bmatrix} \overline{v}(q-1) & \overline{v}(q) & \cdots & \overline{v}(l-1) \\ \overline{v}(q-2) & \overline{v}(q-1) & \cdots & \overline{v}(l-2) \\ \overline{v}(q-3) & \overline{v}(q-2) & \cdots & \overline{v}(l-3) \\ \vdots & \vdots & \ddots & \vdots \\ \overline{v}(0) & \overline{v}(1) & \cdots & \overline{v}(l-q) \end{bmatrix} \in \Re^{(p+m)q\times(l-q+1)}. \tag{8e}$$

Note that the first term in the right-hand side of (8a) represents the effect of the preceding $q-1$ time steps, where $\overline{G}^{q}$ is sufficiently small and all the states in x are bounded [25], so (8a) can be approximated by neglecting the first term $C\overline{G}^{q}x$, such that

$$\overline{y} = \overline{Y}\overline{V}. \tag{9}$$

This has the following least-squares solution:

$$\overline{Y} = \overline{y}\overline{V}^{+}, \tag{10}$$

where $\overline{V}^{+} = \overline{V}^{T}[\overline{V}\overline{V}^{T}]^{-1}$ is the pseudo-inverse matrix of $\overline{V}$. Here, the data length l should be chosen as a sufficiently large integer such that $[\overline{V}\overline{V}^{T}]^{-1}$ exists.

To solve for $\overline{Y}$ uniquely, all the rows of $\overline{V}$ must be linear independent. Furthermore, to minimize any numerical error due to the computation of the pseudo-inverse, the rows of $\overline{V}$ should be chosen as independently as possible. As a result, the maximum value of q is the number that maximizes the number $(p+m)q \leq (l-q+1)$ of independent rows of $\overline{V}$. The maximum q means the upper bound of the order of the deadbeat observer. The lower bound of q must be chosen such that $mq \geq n$, where m is the number of outputs and n is the order of the system. Obviously, q can be smaller than the true order of the system for a multiple output system. For a single output system, the number q must be greater than or equal to the true order of the system.

3.2. Computation of observer Markov parameters

The observer Markov parameters $\overline{Y}_k = C\overline{G}^{k-1}\overline{H}$ include the system Markov parameters $Y_k = CG^{k-1}H$ and the observer gain Markov parameters $Y_k^0 = CG^{k-1}F$. The system Markov parameters and the observer gain Markov parameters are used to combine a Hankel matrix.

3.2.1. System Markov parameters

To recover the system Markov parameters in Y from the observer Markov parameters in $\overline{Y}$, partition $\overline{Y}$ such that

$$\overline{Y} = \left[C\overline{H} \quad C\overline{G}\overline{H} \quad \cdots \quad C\overline{G}^{(q-1)}\overline{H}\right] \triangleq \left[\overline{Y}_1 \quad \overline{Y}_2 \quad \cdots \quad \overline{Y}_q\right], \tag{11a}$$

where

$$\begin{aligned} &\overline{Y}_0 = 0, \\ &\overline{Y}_k = C\overline{G}^{k-1}\overline{H} = \left[C(G+FC)^{k-1}H \quad -C(G+FC)^{k-1}F\right] \\ &\quad \triangleq \left[\overline{Y}_k^{(1)} \quad -\overline{Y}_k^{(2)}\right] \quad \text{for } k = 1, 2, 3, \ldots. \end{aligned} \tag{11b}$$

The system Markov parameters CH of the system can be reformulated as

$$Y_1 = CH = \overline{Y}_1^{(1)}. \tag{12a}$$

To obtain the system Markov parameters CGH, first consider the product $\overline{Y}_2^{(1)}$ as

$$\overline{Y}_2^{(1)} = C(G+FC)H = CGH + CFCH = Y_2 + \overline{Y}_1^{(2)}Y_1.$$

Hence, one has

$$Y_2 = CGH = \overline{Y}_2^{(1)} - \overline{Y}_1^{(2)} Y_1. \tag{12b}$$

Similarly, to obtain the system Markov parameters CG^2H, consider the product $\overline{Y}_3^{(1)}$

$$\begin{aligned}\overline{Y}_3^{(1)} &= C(G + FC)^2 H \\ &= CG^2H - (CF)CGH - C(G + FC)F(CH) \\ &= Y_3 + \overline{Y}_1^{(2)} Y_2 + \overline{Y}_2^{(2)} Y_1\end{aligned}$$

Then, one has

$$Y_3 = CG^2H = \overline{Y}_3^{(1)} - \overline{Y}_1^{(2)} Y_2 - \overline{Y}_2^{(2)} Y_1. \tag{12c}$$

By induction, the general relationship between the system Markov parameters Y_k and the observer Markov parameters $\overline{Y}_k$ is

$$Y_0 = \overline{Y}_0 = 0, \tag{13a}$$

$$Y_k = \overline{Y}_k^{(1)} - \sum_{i=1}^{k} \overline{Y}_i^{(2)} Y_{k-i} \quad \text{for } k = 1, 2, \ldots, q, \tag{13b}$$

$$Y_k = -\sum_{i=1}^{q} \overline{Y}_i^{(2)} Y_{k-i} \quad \text{for } k = q+1, \ldots, \infty. \tag{13c}$$

3.2.2. Observer gain Markov parameters

To identify the observer gain F, first recovers the sequence of parameters as follows:

$$Y_k^0 = CG^{k-1}F \quad \text{for } k = 1, 2, 3, \ldots. \tag{14a}$$

In terms of the observer gain Markov parameters. In fact, the first parameter of Eq. (14a) in the sequence is

$$Y_1^0 = CF = \overline{Y}_1^{(2)}. \tag{14b}$$

The next parameter in the sequence is obtained by considering $\overline{Y}_2^{(2)}$

$$\begin{aligned}\overline{Y}_2^{(2)} &= C\overline{G}F = (CGF + CFCF) \\ &= Y_2^0 + \overline{Y}_1^{(2)} Y_1^0.\end{aligned}$$

Then, one has

$$Y_2^0 = CGF = \overline{Y}_2^{(2)} - \overline{Y}_1^{(2)} Y_1^0. \tag{14c}$$

Similarly, one gets

$$\overline{Y}_3^{(2)} = C\overline{G}^2F = (CG^2F + CFCGF + C\overline{G}FCF) = Y_3^0 + \overline{Y}_1^{(2)} Y_2^0 + \overline{Y}_2^{(2)} Y_1^0.$$

Then, one has

$$Y_3^0 = CG^2F = \overline{Y}_3^{(2)} - \overline{Y}_1^{(2)} Y_2^0 - \overline{Y}_2^{(2)} Y_1^0. \tag{14d}$$

The general relationship can be summarized as follows:

$$Y_1^0 = CF = \overline{Y}_1^{(2)}, \tag{15a}$$

$$Y_k^0 = \overline{Y}_k^{(2)} - \sum_{i=1}^{k-1} \overline{Y}_i^{(2)} Y_{k-i}^0 \quad \text{for } k = 2, 3, \ldots, q, \tag{15b}$$

$$Y_k^0 = -\sum_{i=1}^{q} \overline{Y}_i^{(2)} Y_{k-i}^0 \quad \text{for } k = q+1, \ldots, \infty. \tag{15c}$$

3.3. Eigensystem realization algorithm

The Hankel matrix $\hat{H}(k-1)$ from the combined observer Markov parameters is associated with the system and observer as

$$\hat{H}(k-1) = \begin{bmatrix} \Upsilon_k & \Upsilon_{k+1} & \cdots & \Upsilon_{k+\beta-1} \\ \Upsilon_{k+1} & \Upsilon_{k+2} & \cdots & \Upsilon_{k+\beta} \\ \vdots & \vdots & \ddots & \vdots \\ \Upsilon_{k+\alpha-1} & \Upsilon_{k+\alpha} & \cdots & \Upsilon_{k+\alpha+\beta-2} \end{bmatrix}, \tag{16}$$

where $\alpha \geq 0$ and $\beta \geq 0$ are sufficiently large arbitrary integers and $\Upsilon_k = [\ Y_k \quad Y_k^0\ ] = [\ CG^{k-1}H \quad CG^{k-1}F\ ]$. When the combined observer Markov parameters are determined, the eigensystem realization algorithm (ERA) method is used to obtain the desired discrete system realization $[G, H, C, F]$ through singular value decomposition (SVD) of the Hankel matrix.

The ERA processes the factorization of the block data matrix in Eq. (16), started for $k = 1$, using the singular value decomposition $\hat{H}(0) = V \sum S^T$, where the columns of matrices V and S are orthonormal and $\sum$ is a rectangular matrix of the form as follows

$$\sum = \begin{bmatrix} \sum_{\tilde{n}} & 0 \\ 0 & 0 \end{bmatrix}, \tag{17}$$

where $\sum_{\tilde{n}} = diag[\sigma_1, \sigma_2, \ \ldots, \sigma_{n_{\min}}, \sigma_{n_{\min}+1}, \ \ldots, \sigma_{\tilde{n}}\ ]$ contains monotonically non-increasing entries $\sigma_1 \geq \sigma_2 \geq \cdots \geq \sigma_{n_{\min}} \geq \sigma_{n_{\min}+1} \geq \cdots \sigma_{\tilde{n}} \geq 0$. Here, some singular values $(\sigma_{n_{\min}+1}, \ldots, \sigma_{\tilde{n}})$ are relatively small $(\sigma_{n_{\min}+1} \ll \sigma_{n_{\min}})$ and negligible in the sense that they contain more noise information than system information. In order to construct the low-order observer of the system, lets define $\sum_{n_{\min}} = diag[\sigma_1, \sigma_2, \ \ldots, \sigma_{n_{\min}}]$. In other words, the reduced model of order $n_{\min}$ after deleting singular values $(\sigma_{n_{\min}+1}, \ldots, \sigma_{\tilde{n}})$ is then considered as the robustly controllable and observable part of the realized system with an acceptable closed-loop performance. Simultaneous realizations of the system and observer by the ERA are given as

$$G = \sum_{n_{\min}}^{-1/2} V_{n_{\min}}^T \hat{H}(1) S_{n_{\min}} \sum_{n_{\min}}^{-1/2}, \tag{18a}$$

$$\begin{bmatrix} H & F \end{bmatrix} = \text{First } (m+p) \text{ columns of } \sum_{n_{\min}}^{1/2} S_{n_{\min}}^T, \tag{18b}$$

$$C = \text{ First } p \text{ rows of } V_{n_{\min}} \sum_{n_{\min}}^{1/2}. \tag{18c}$$

For system identification, SVD is very useful in determining the system order. In practice, the primary purpose of applying the OKID method is that the constructed observer satisfies the least-squares solution or acts the input–output map the same as a Kalman filter. If the data length is sufficiently long and the order of the observer is sufficiently large, the truncation error is negligible [18].

The procedure of performing the off-line system identification scheme to obtain both system and observer gain Markov parameters of the OKID model is given as follows, and the flowchart is illustrated in Fig. 1.

(i) Compute the observer Markov parameters. Choose a value of q that determines the number of observer Markov parameters from the given set of input–output data, and then compute the least-squares solution of the observer Markov parameter matrix $\overline{Y}$ in (10).
(ii) Recover system and observer gain Markov parameters. Based on the observer Markov parameters identified in (i), use (13) and (15) to determine the combined system and observer gain Markov parameters. Moreover, set up the Hankel matrix $\hat{H}(0)$ and $\hat{H}(1)$ as shown in (16).
(iii) Realize a state-space model $\begin{bmatrix} G, & H, & C \end{bmatrix}$ and the corresponding observer gain F in (18) from the identified sequence of the system and observer gain Markov parameters by using the ERA method.

3.4. Relationship to Kalman filter

Let system Eq. (2) be extended to include process and measurement noise described as

$$x(k+1) = Gx(k) + Hu(k) + w(k), \tag{19a}$$

$$y(k) = Cx(k) + v(k), \tag{19b}$$

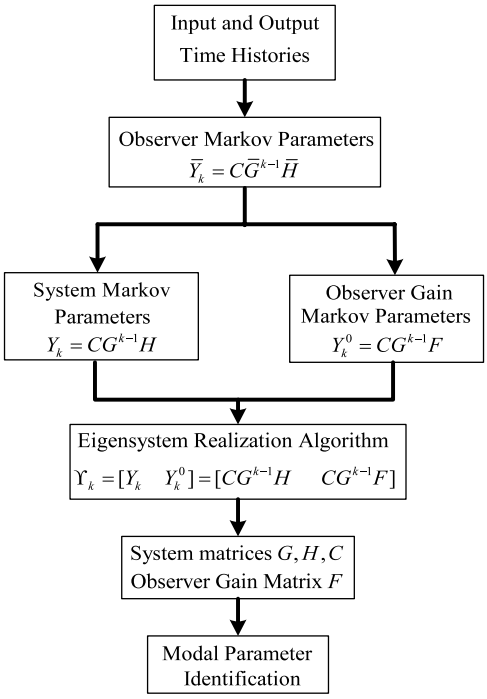

Fig. 1. Flowchart of the OKID.

where $w(k)$ is the process noise assumed to be Gaussian, zero-mean and white with the covariance matrix Q and $v(k)$ is the measurement noise satisfies the same assumption as $w(k)$ with a different covariance matrix $\mathbb{R}$. The sequences $w(k)$ and $v(k)$ are independent of each other. Then, a typical Kalman filter for system (19) can be written as

$$\hat{x}(k+1) = G\hat{x}(k) + Hu(k) + K\varepsilon_r(k), \tag{20a}$$

$$\hat{y}(k) = C\hat{x}(k), \tag{20b}$$

where $\hat{x}(k)$ is the estimated state, K is the Kalman filter gain, and $\varepsilon_r(k)$ is defined as the difference between the real measurement $y(k)$ and the estimated measurement $\hat{y}(k)$. Combination of systems (19) and (20) yields

$$\begin{aligned}\hat{x}(k+1) &= G\hat{x}(k) + Hu(k) + K[y(k) - C\hat{x}(k)] \\ &= \widetilde{G}\hat{x}(k) + \widetilde{H}\widetilde{v}(k),\end{aligned} \tag{21a}$$

where $\widetilde{G} = G - KC$, $\widetilde{H} = [\,H, \quad K\,]$, $\widetilde{v}(k) = \begin{bmatrix} u(k) \\ y(k) \end{bmatrix}$.

The measurement equation becomes

$$y(k) = \hat{y}(k) + \varepsilon_r(k) = C\hat{x}(k) + \varepsilon_r(k). \tag{21b}$$

Systems (5) and (21) are identical when $F = -K$ and $\varepsilon_r(k) = 0$, and so are Markov parameters. In practice, any observer satisfying a least-squares solution will produce the same input–output map as a Kalman filter does, provided that the data length is sufficiently long and the order of the Hankel matrix is sufficiently large, so that the truncation error is negligible [18]. Therefore, when the residual $\varepsilon_r(k)$ is a white sequence of the Kalman filter residual, the observer gain F converges to the steady-state Kalman filter gain K such that $F = -K$.

4. The prediction-based digital redesign

4.1. Linear quadratic analog tracker design

Consider a linear quadratic analog system described as

$$\dot{x}_c(t) = Ax_c(t) + Bu_c(t), \tag{22a}$$

$$y_c(t) = Cx_c(t), \qquad x_c(0) = x_0, \tag{22b}$$

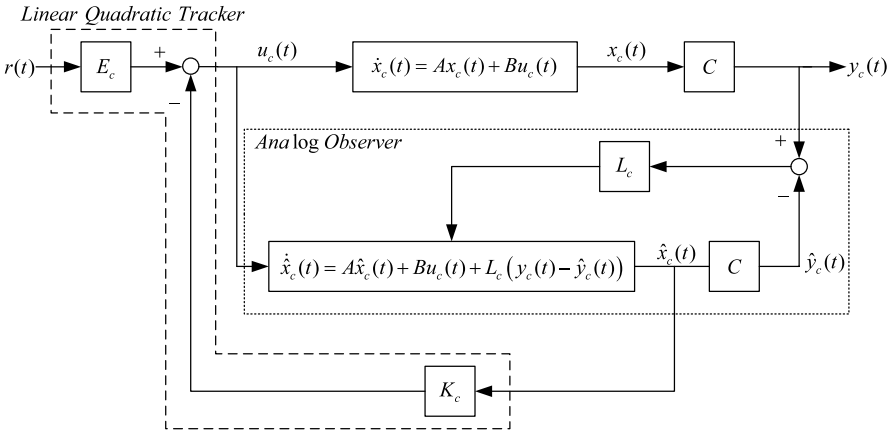

Fig. 2. Observer-based linear quadratic analog tracker.

which is assumed to be both controllable and observable, $x_c(t) \in \Re^n$, $u_c(t) \in \Re^m$ and $y_c(t) \in \Re^p$. The optimal quadratic state-feedback control law is to minimize the following performance index:

$$J = \int_0^\infty \left\{ [\, Cx_c(t) - r(t)\,]^T\, Q\, [Cx_c(t) - r(t)\,] + u_c^T(t) R u_c(t) \right\} \mathrm{d}t, \tag{23}$$

with $Q \geq 0$ and $R > 0$. This optimal control is given by

$$u_c(t) = -K_c x_c(t) + E_c r(t). \tag{24}$$

Then, the resulting closed-loop system becomes

$$\dot{x}_c(t) = (A - BK_c)x_c(t) + BE_c r(t), \tag{25}$$

where the analog feedback gain $K_c \in \Re^{m\times n}$ and the forward gain $E_c \in \Re^{m\times m}$ for $m = p$ are

$$K_c = R^{-1}B^T P, \tag{26}$$

$$E_c = -R^{-1}B^T[(A - BK_c)^{-1}]^T C^T Q. \tag{27}$$

Here, $r(t)$ is a reference input or desired trajectory, and P is the positive definite and symmetric solution of the following Riccati equation as

$$A^T P + PA - PBR^{-1}B^T P + C^T QC = 0. \tag{28}$$

The closed-loop system (25) is asymptotically due to the property of LQR (23) design.

4.2. Observer-based linear quadratic analog tracker design

Consider the situation that the system state of system (22) cannot all be measured. Then, one can take advantage of the observer to estimate the unmeasured system state. Consider the linear observable continuous-time system in Fig. 2, which is described as follows

$$\dot{\hat{x}}_c(t) = A\hat{x}_c(t) + Bu_c(t) + L_c[y_c(t) - C\hat{x}_c(t)], \tag{29}$$

where $\hat{x}_c(t)$ is the estimate of $x_c(t)$ and $L_c \in \Re^{n\times p}$ is the observer gain.

To demonstrate that the proposed dynamical system (29) is indeed an observer, it is necessary to show that it manufactures an estimate $\hat{x}_c(t)$ that is close to the actual state $x_c(t)$, i.e., $\hat{x}_c(t) \approx x_c(t)$. First, let the estimation error be

$$\widetilde{x}_c(t) = x_c(t) - \hat{x}_c(t), \tag{30}$$

which implies

$$\dot{\widetilde{x}}_c(t) = \dot{x}_c(t) - \dot{\hat{x}}_c(t). \tag{31}$$

Substituting (22), (29) and (30) into (31) yields

$$\dot{\widetilde{x}}_c(t) = (A - L_c C)\widetilde{x}_c(t), \tag{32}$$

which contrasts (25) and (32) with $r(t) = 0$. One can see that

$$(A - L_c C)^T = A^T - C^T L_c^T. \tag{33}$$

This has the same structure as a state-feedback controller (25). With the dual property of linear system, the optimal observer gain L_c can be found from designing the optimal control gain K_c. It means that the same theory one have developed for selecting the analog-feedback gain K_c can be used to select the observer gain L_c as follows

$$L_c = P_o C^T R_o^{-1}, \tag{34}$$

where P_o is the symmetric and positive definite solution of the following Riccati equation as

$$AP_o + P_o A^T - P_o C^T R_o^{-1} C P_o + Q_o = 0, \tag{35}$$

in which $Q_o \geq 0$ and $R_o > 0$ with appropriate dimensions.

It is well known that the high-gain (analog) controller/observer induces a high quality performance on trajectory tracking design/state estimation, and it also can suppress system uncertainties such as nonlinear perturbations, parameter variations, modeling errors and external disturbances. For these reasons, the sub-optimal analog controller and observer with a high-gain property is adopted in our approach. The high-gain property controller can be obtained by choosing a sufficiently high ratio of Q to R in (28) so that the system output can closely track the pre-specified trajectory. However, the high-gain property of the analog tracker usually yields large control signals, which might cause the system actuator to saturate and give unsatisfactory system response. To overcome this difficulty, the tracker is redesigned based on the advanced digital-redesign technique equipped with a suitably large sampling period and zero hold, which yields an equivalent digital controller but with a low gain, without possibly losing the high quality performance. However, a large sampling period usually induces a degradation of the tracking performance. Therefore, in general, a suitable compromise between the pre-specified performance and the selections of the sampling time T_s, weighting matrices (Q_o, R_o) in (35) and (Q, R) in (28) should be considered. For simplicity in discussion, we neglect the actuator saturation problem in this thesis.

4.3. Digital redesign of the linear quadratic analog tracker

The continuous-time state-feedback controller is

$$u_c(t) = -K_c x_c(t) + E_c r(t), \tag{36}$$

where $K_c \in \Re^{m\times n}$ and $E_c \in \Re^{n\times m}$ have been designed to satisfy some specified goals, and $r(t) \in \Re^m$ is a desired reference input vector. Thus, the analogously controlled system is

$$\dot{x}_c(t) = A_c x_c(t) + B E_c r(t), \qquad x_c(0) = x_{c0} = x_0, \tag{37}$$

where $A_c = A - BK_c$. Let the state equation of a corresponding discrete-time equivalent model be

$$\dot{x}_d(t) = A x_d(t) + B u_d(t), \quad x_d(0) = x_{d0} = x_0, \tag{38}$$

where $u_d(t) \in \Re^m$ is a piecewise-constant input vector, satisfying

$$u_d(t) = u_d(kT_s), \quad \text{for } kT_s \leq t < (k+1)T_s,$$

and $T_s > 0$ is the sampling period. Then, the discrete-time state-feedback controller is given by [17] as

$$u_d(kT_s) = -K_d x_d(kT_s) + E_d\, r^*(kT_s), \tag{39}$$

where

$$K_d = (I_m + K_c H)^{-1} K_c G, \tag{40}$$

$$E_d = (I_m + K_c H)^{-1} E_c, \tag{41}$$

$$r^*(kT_s) = r(kT_s + T_s), \tag{42}$$

$$G = \mathrm{e}^{AT_s}, \tag{43}$$

$$H = (G - I_n)A^{-1}B \quad \text{for nonsingular } A, \tag{44a}$$

$$H = \left[T_s I_n + A\frac{(T_s)^2}{2!} + A^2\frac{(T_s)^3}{3!} + \cdots\right] B \quad \text{for singular } A, \tag{44b}$$

$K_d \in \Re^{m\times n}$ is a digital state-feedback gain, $E_d \in \Re^{m\times m}$ is a digital feed forward gain, and $r^*(kT_s) \in \Re^m$ is a piecewise-constant reference input vector determined in terms of $r(kT_s)$ for tracking purpose. Thus, the digitally controlled closed-loop system becomes

$$\dot{x}_d(t) = A x_d(t) + B\,[-K_d x_d(kT_s) + E_d r^*(kT_s)], \tag{45}$$

where $x_d(0) = x_{d0}$, for $kT_s \leq t < (k+1)T_s$.

Remark 1 (*Sampling Period Selection*)**.** It is noted that the mapping of a continuous-time system to its corresponding discredited system can be one-to-one if the selected sampling period satisfies the sampling theorem [26]. However, if a sampling period that violates the sampling theorem is selected, then the satisfactory state-matching will not be achieved. Hence, it is suggested to choose T_s such that $T_s < \min(\pi / \mathrm{Im}(\lambda(A - BK_c)))$ and $T_s < \min(\pi / \mathrm{Im}(\lambda(A - L_cC)))$, where $\mathrm{Im}(\cdot)$ denotes the imaginary part of $(\cdot)$, to obtain an acceptable state-matching performance.

4.4. Digital redesign of the observer-based linear quadratic analog tracker

Consider the linear continuous-time observer as follows:

$$\dot{\hat{x}}_c(t) = A\hat{x}_c(t) + Bu_c(t) + L_c[y_c(t) - C\hat{x}_c(t)]. \tag{46}$$

Define the continuous-time error $\widetilde{x}_c(t)$ and discrete-time state estimate error $\widetilde{x}_d(kT_s)$ respectively as

$$\begin{aligned} &\widetilde{x}_c(t) \equiv x_c(t) - \hat{x}_c(t), \\ &\widetilde{x}_d(kT_s) \equiv x_d(kT_s) - \hat{x}_d(kT_s). \end{aligned} \tag{47}$$

The aim of digital redesign is to make the discrete-time state estimation error closely match the continuous-time state estimation error at each sampling instant, such as

$$\widetilde{x}_d(kT_s) \approx \widetilde{x}_c(t)\,\big|_{t=kT_s}\ .$$

Using the duality once again, one can find the discrete-time state estimation error dynamics as follows

$$\widetilde{x}_d(kT_s + T_s) = (G - MN)\,\widetilde{x}_d(kT_s), \tag{48}$$

where

$$G = \mathrm{e}^{AT_s}, \tag{49}$$

$$M = (G - I_n)A^{-1}L_c \quad \text{for nonsingular } A, \tag{50a}$$

$$M = \left[T_sI_n + A\frac{(T_s)^2}{2!} + A^2\frac{(T_s)^3}{3!} + \cdots\right]L_c \quad \text{for singular } A, \tag{50b}$$

$$N = (I_m + CM)^{-1}CG. \tag{51}$$

Further define

$$L_d = M(I_m + CM)^{-1}, \tag{52}$$

then one has

$$MN = (G - I_n)A^{-1}L_c(I_m + CM)^{-1}CG = L_dCG. \tag{53}$$

The discrete-time system [26] corresponding to the analog system (22) are shown as

$$x_d(kT_s + T_s) = Gx_d(kT_s) + Hu_d(kT_s), \tag{54a}$$

$$y_d(kT_s) = Cx_d(kT_s). \tag{54b}$$

From (54), one has

$$CGx_d(kT_s) = Cx_d(kT_s + T_s) - CH\,u_d(kT_s) = y_d(kT_s + T_s) - CH\,u_d(kT_s). \tag{55}$$

Substituting (53) into (48) yields

$$\begin{aligned} \widetilde{x}_d(kT_s + T_s) &= (G - L_dCG)(x_d(kT_s) - \hat{x}_d(kT_s)) \\ &= (G - L_dCG)x_d(kT_s) - (G - L_dCG)\hat{x}_d(kT_s). \end{aligned} \tag{56}$$

Substituting (55) into (56), one has

$$\begin{aligned} \widetilde{x}_d(kT_s + T_s) &= x_d(kT_s + T_s) - \hat{x}_d(kT_s + T_s) \\ &= [Gx_d(kT_s) + Hu_d(kT_s)] - \hat{x}_d(kT_s + T_s) \\ &= Gx_d(kT_s) - L_d[y_d(kT_s + T_s) - CHu_d(kT_s)] - (G - L_dCG)\hat{x}_d(kT_s) \\ &= Gx_d(kT_s) - L_dy_d(kT_s + T_s) + L_dCHu_d(kT_s) - (G - L_dCG)\hat{x}_d(kT_s). \end{aligned} \tag{57}$$

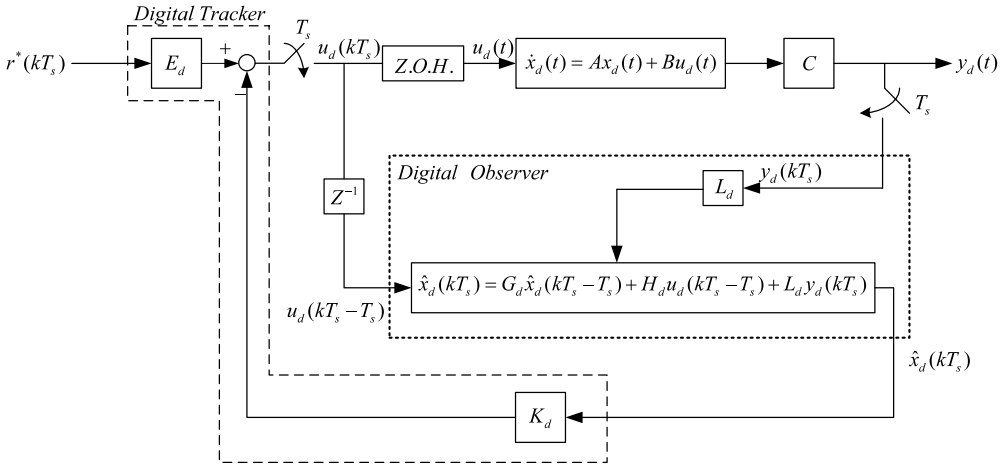

Fig. 3. Prediction-based digital tracker and observer.

From (57), one has

$$\begin{aligned}\hat{x}_d(kT_s + T_s) &= (G - L_d CG)\,\hat{x}_d(kT_s) + (I_n - L_d C)\,H\,u_d(kT_s) + L_d y_d(kT_s + T_s)\\ &= G_d\,\hat{x}_d(kT_s) + H_d\,u_d(kT_s) + L_d y_d(kT_s + T_s),\end{aligned} \tag{58a}$$

$$\hat{y}_d(kT_s) = C\,\hat{x}_d(kT_s), \tag{58b}$$

where

$$L_d = (G - I_n)A^{-1}L_c\,(I_m + C(G - I_n)A^{-1}L_c)^{-1}, \tag{59}$$

$$G_d = G - L_d CG, \tag{60}$$

$$H_d = (I_n - L_d C)H, \tag{61}$$

$$G = \mathrm{e}^{AT_s}, \tag{62}$$

$$H = (G - I_n)A^{-1}B \quad \text{for nonsingular } A, \tag{63a}$$

$$H = \left[T_s I_n + A\frac{(T_s)^2}{2!} + A^2\frac{(T_s)^3}{3!} + \cdots\right]B \quad \text{for singular } A. \tag{63b}$$

Note that the digital observer (58a) utilizes the future sampled output $y_d(kT_s + T_s)$ together with the currently estimated state $\hat{x}_d(kT_s)$ to compute the future estimated state $\hat{x}_d(kT_s + T_s)$. In view of practical implementation, the following discrete observer using currently output $y_d(kT_s)$ and previous estimated state $\hat{x}_d(kT_s - T_s)$ to compute the currently estimated state $\hat{x}_d(kT_s)$ as follows:

$$\hat{x}_d(kT_s) = G_d\,\hat{x}_d(kT_s - T_s) + H_d\,u_d(kT_s - T_s) + L_d y_d(kT_s), \tag{64a}$$

$$\hat{y}_d(kT_s) = C\,\hat{x}_d(kT_s). \tag{64b}$$

The observer-based digital tracker and observer for the sampled-data linear model are shown in Fig. 3.

5. Design procedure

In this section, the design procedure of the proposed method is listed as the following steps:

Step 1. Perform the off-line observer/Kalman filter identification (OKID) method to determine appropriate (low) orders of the linear system/observer models and system matrices/observer gain matrix, in the general coordinate form.

Step 2. Transform the obtained discrete-time linear system/observer models to continuous time linear system/observer models with the appropriate sampling time.

Step 3. Design the linear quadratic analog tracker and the analog observer form the continuous time linear system/observer models obtained in Step 2.

Step 4. Perform the digital redesign on the linear quadratic tracker and the analog observer obtained in Step 3. The digital redesign of the observer-based linear quadratic analog tracker is shown in Fig. 4a for Type 1: the interconnected terms go through zero-order-hold (Z.O.H.) and in Fig. 4b for Type 2: the interconnected terms do not go through zero-order-hold. And the proposed method is work for both Types.

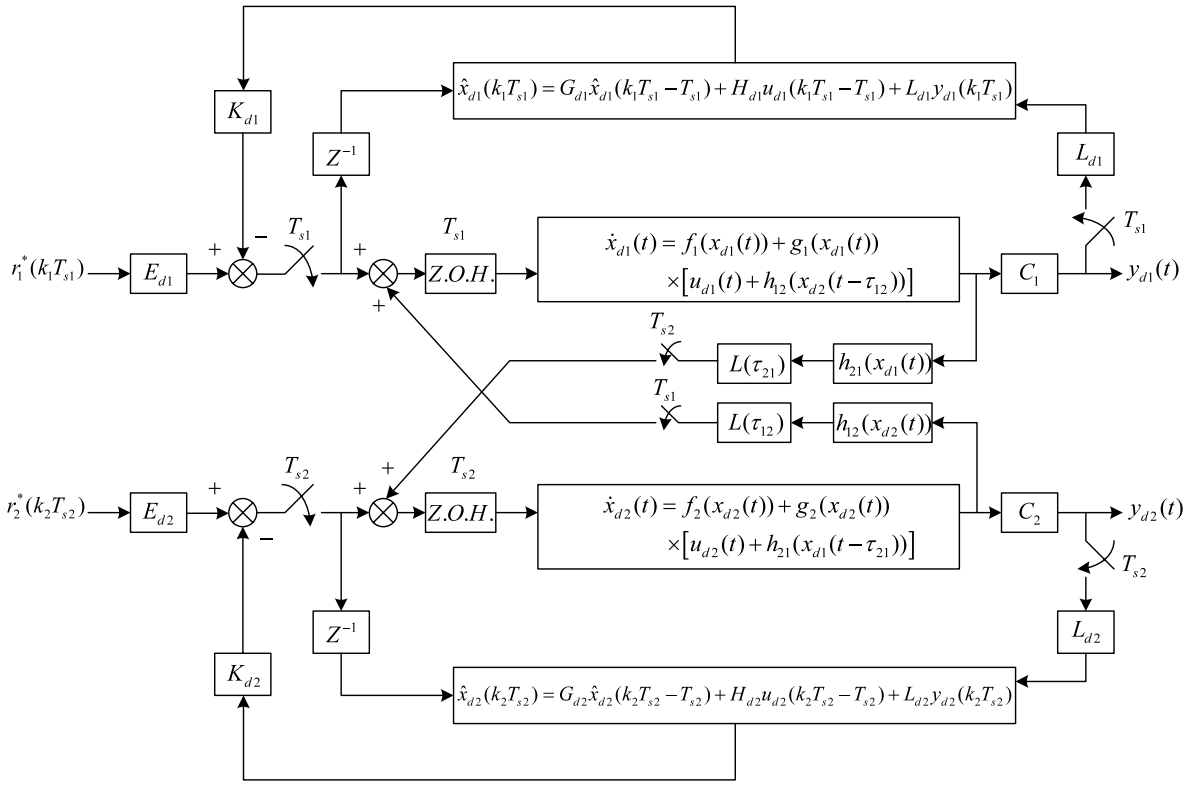

Fig. 4a. The decentralized observer-based digital-redesigned tracker for the unknown nonlinear sampled-data system with Type 1 interconnection.

Remark 2. Let the linear case of Subsystem Σ_1 in Fig. 4b be

$$\dot{x}_{d1}(t) = A_1x_{d1}(t) + B_1[u_{d1}(t) + h_{12}x_{d2}(t - \tau_{12})]. \tag{65}$$

The solutions $X_1(s)$ and $x_1(t)$ of (65) are respectively given as

$$X_{d1}(s) = (sI - A)^{-1}x_{d1}(0) + (sI - A)^{-1}B_1U_{d1}(s) + (sI - A)^{-1}B_1h_{12}X_{d2}(s)e^{-\tau_{12}s}$$

and

$$x_{d1}(t) = e^{At}x_{d1}(0) + e^{At} \otimes B_1u_{d1}(t) + e^{At} \otimes B_1h_{12}x_{d2}(t - \tau_{12}),$$

where $\otimes$ denotes the convolution operator. It is not easy to find the corresponding discrete-time model of (65), if the interconnected term $h_{12}x_{d2}(t - \tau_{12})$ does not going though the zero-order-hold. However, by the proposed approach, one always can have the optimal linear discrete-time model by the eigensystem realization algorithm (ERA).

6. Illustrative examples

6.1. A MIMO large-scale unknown linear system

Consider the large-scale unknown system that contains two interconnected two-in-two-out subsystems described as follows:

$$\Sigma_1 : \dot{x}_1(t) = A_1x_1(t) + B_1\left[u_1(t) + L_{12}x_2(t - \tau_{12})\right]; \qquad y_1(t) = C_1x_1(t), \tag{66}$$

$$\Sigma_2 : \dot{x}_2(t) = A_2x_2(t) + B_2\left[u_2(t) + L_{21}x_1(t - \tau_{21})\right]; \qquad y_2(t) = C_2x_2(t), \tag{67}$$

where $u_1(t) = \begin{bmatrix} u_{1,1}(t) \\ u_{1,2}(t) \end{bmatrix}$, $u_2(t) = \begin{bmatrix} u_{2,1}(t) \\ u_{2,2}(t) \end{bmatrix}$, $x_1(t) = \begin{bmatrix} x_{1,1}(t) \\ x_{1,2}(t) \\ x_{1,3}(t) \end{bmatrix}$, $x_2(t) = \begin{bmatrix} x_{2,1}(t) \\ x_{2,2}(t) \\ x_{2,3}(t) \end{bmatrix}$, $A_1 = \begin{bmatrix} -3 & 5 & 9 \\ 1 & -5 & 3 \\ -2 & 8 & -2 \end{bmatrix}$, $A_2 = \begin{bmatrix} -2 & 1 & -2 \\ -2 & 1 & -1 \\ 0 & -3 & -4 \end{bmatrix}$, $B_1 = \begin{bmatrix} 2 & -1 \\ 1 & 0 \\ 0 & -1 \end{bmatrix}$, $B_2 = \begin{bmatrix} 1 & 0 \\ -1 & -2 \\ -2 & 0 \end{bmatrix}$, $C_1 = \begin{bmatrix} 0 & 1 & 0 \\ 0 & 0 & 1 \end{bmatrix}$, $C_2 = \begin{bmatrix} 1 & 0.1 & 0 \\ 0 & 1 & 0 \end{bmatrix}$, $L_{12} = \begin{bmatrix} 2 & 0 & 2 \\ 0 & 2 & 0 \end{bmatrix}$, $L_{21} = \begin{bmatrix} 0 & 2 & 0 \\ 0 & 0 & 2 \end{bmatrix}$ and the initial condition $x_1(0) = \begin{bmatrix} 0 \\ 0 \\ 0 \end{bmatrix}$, $x_2(0) = \begin{bmatrix} 0 \\ 0 \\ 0 \end{bmatrix}$, $\tau_{21} = 2 \times T_{s1}$, $\tau_{12} = 3 \times T_{s2}$, where $T_{s1} = 0.01$ s and $T_{s2} = 0.02$ s.

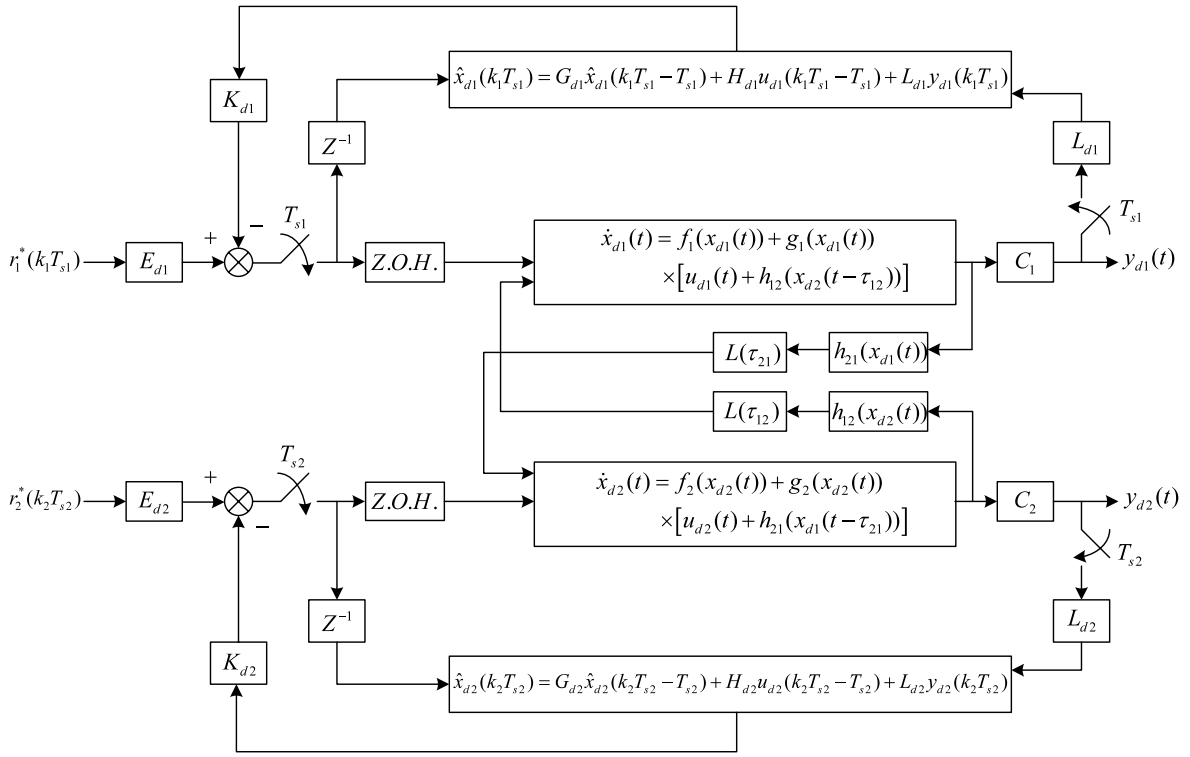

Fig. 4b. The decentralized observer-based digital-redesigned tracker for the unknown nonlinear sampled-data system with Type 2 interconnection.

Let the system be excited by the white-noise control force $u(t) = \begin{bmatrix} u_1(t) & u_2(t) \end{bmatrix}^T$ with a zero mean and covariance $diag\,[cov(u_1(t)), cov(u_2(t))] = diag\begin{bmatrix} 0.2 & 0.2 \end{bmatrix}$, where the sampling times are $T_{s1} = 0.01$ s and $T_{s2} = 0.02$ s for Subsystem Σ_1 and Subsystem Σ_2, respectively. The input–output sampled data are given in Fig. 5.

The identified system and observer gain matrices for Subsystem Σ_1 and Subsystem Σ_2 are respectively given as

$$\hat{G}_1 = \begin{bmatrix} 1.1911 & -0.1154 & 0.0553 & 0.0186 \\ 0.1580 & 1.0151 & -0.0091 & -0.1210 \\ -0.1349 & -0.0118 & 0.9068 & 0.0470 \\ 0.0222 & 0.2306 & -0.0590 & 0.7377 \end{bmatrix}, \quad \hat{H}_1 = \begin{bmatrix} -0.0052 & 0.0032 \\ -0.0094 & 0.0029 \\ 0.0014 & -0.0043 \\ -0.0092 & 0.0027 \end{bmatrix},$$

$$\hat{C}_1 = \begin{bmatrix} 0.3794 & -0.8012 & -0.5613 & -0.5576 \\ -0.9758 & -1.0536 & 0.6339 & -0.4554 \end{bmatrix}, \quad F_1 = \begin{bmatrix} -2.5749 & 2.1314 \\ 1.8075 & 0.7548 \\ -0.5690 & 0.9213 \\ -0.6070 & -0.4564 \end{bmatrix},$$

$$\hat{G}_2 = \begin{bmatrix} 1.1530 & -0.0175 & -0.0657 & 0.0432 \\ 0.0254 & 1.1083 & -0.0542 & 0.0695 \\ -0.1500 & 0.1101 & 0.8802 & 0.0027 \\ -0.0918 & -0.1598 & -0.0020 & 0.8565 \end{bmatrix}, \quad \hat{H}_2 = \begin{bmatrix} -0.0122 & -0.0145 \\ 0.0030 & -0.0123 \\ 0.0145 & 0.0103 \\ 0.0060 & 0.0206 \end{bmatrix},$$

$$\hat{C}_2 = \begin{bmatrix} -0.5218 & 0.9971 & 0.7799 & -0.3849 \\ 0.9543 & 0.5403 & -0.3939 & -0.7613 \end{bmatrix}, \quad F_2 = \begin{bmatrix} 1.2978 & -2.3511 \\ -2.2092 & -1.1693 \\ 0.9099 & -0.5030 \\ -0.4717 & -0.8778 \end{bmatrix}.$$

Then, the observer-based outputs compared with the actual system outputs for Subsystem Σ_1 are shown in Fig. 6, and Subsystem Σ_2 has similar simulation results.

To overcome the effect of modeling error, an improved observer with the high-gain property based on the digital-redesign approach has been used in (65), where the observer system matrices and observer gain matrices with digital redesign for Subsystem Σ_1 and Subsystem Σ_2 are respectively given as

$$G_{d1} = \left(I_n - L_{d1}\hat{C}_1\right)\hat{G}_1 = \begin{bmatrix} -0.0864 & -0.2293 & 0.7518 & 0.0998 \\ -0.0236 & 0.0480 & -0.1313 & -0.3993 \\ -0.1202 & -0.2523 & 0.8425 & -0.0275 \\ 0.0887 & 0.0415 & -0.1406 & 0.6740 \end{bmatrix},$$

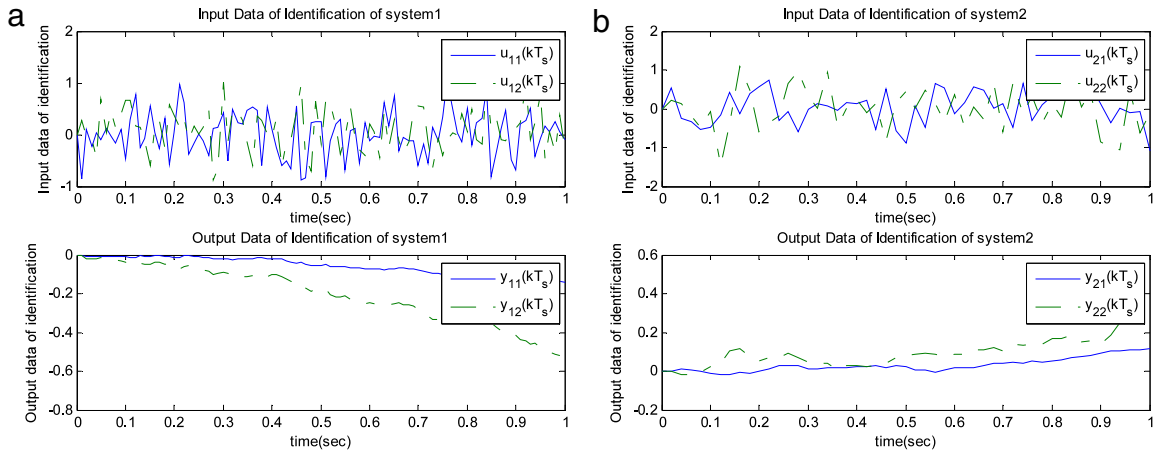

Fig. 5. (a) Subsystem Σ_1 I/O data for identification, (b) Subsystem Σ_2 I/O data for identification.

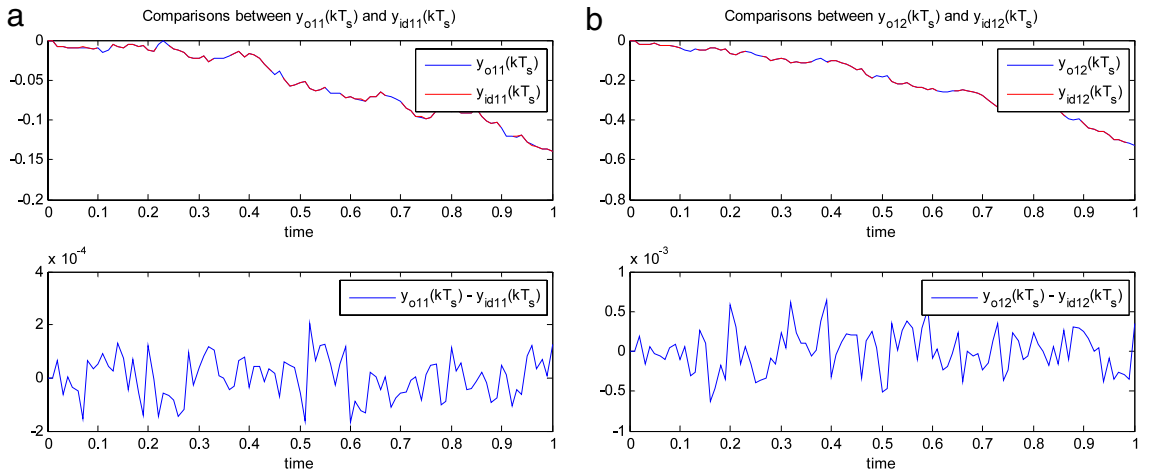

Fig. 6. (a) The comparison between Subsystem Σ_1 output $y_{id11}(kT_s)$ and its observer-based output $y_{o11}(kT_s)$ by OKID, (b) The comparison between Subsystem Σ_1 output $y_{id12}(kT_s)$ and its observer-based output $y_{o12}(kT_s)$ by OKID.

$$H_{d1} = (I_n - L_{d1}\hat{C}_1)\hat{H}_1 = \begin{bmatrix} 0.0026 & -0.0039 \\ 0.0031 & -0.0003 \\ 0.0043 & -0.0048 \\ -0.0072 & 0.0027 \end{bmatrix}, \qquad L_{d1} = \begin{bmatrix} 0.6650 & -0.7153 \\ -0.6536 & -0.3058 \\ -0.1978 & -0.0436 \\ -0.1880 & -0.0046 \end{bmatrix},$$

with $Q_{ob1} = 10^8 \times I_4$, $R_{ob1} = I_2$.

$$G_{d2} = \left(I_n - L_{d2}\hat{C}_2\right)\hat{G}_2 = \begin{bmatrix} -0.0428 & -0.0063 & 0.5397 & 0.3610 \\ 0.0172 & -0.0232 & -0.3557 & 0.4824 \\ -0.0608 & 0.0136 & 0.8190 & 0.0137 \\ -0.0150 & -0.0342 & 0.0015 & 0.7903 \end{bmatrix},$$

$$H_{d2} = (I_n - L_{d2}\hat{C}_2)\hat{H}_2 = \begin{bmatrix} 0.0104 & 0.0139 \\ -0.0021 & 0.0060 \\ 0.0124 & 0.0098 \\ 0.0052 & 0.0168 \end{bmatrix}, \qquad L_{d2} = \begin{bmatrix} -0.4012 & 0.7495 \\ 0.6995 & 0.3768 \\ 0.0892 & -0.0244 \\ -0.0526 & -0.0895 \end{bmatrix},$$

with $Q_{ob2} = 10^8 \times I_4$, $R_{ob2} = I_2$. Then, the comparisons between the actual outputs and their observer-based outputs by digital redesign for Subsystem Σ_1 are shown in Fig. 7, and certainly the results for Subsystem Σ_2 are similar to Σ_1.

By the identified linear models, the observer-based digital-redesigned tracker can be used to design the decentralized control as shown in Fig. 8.

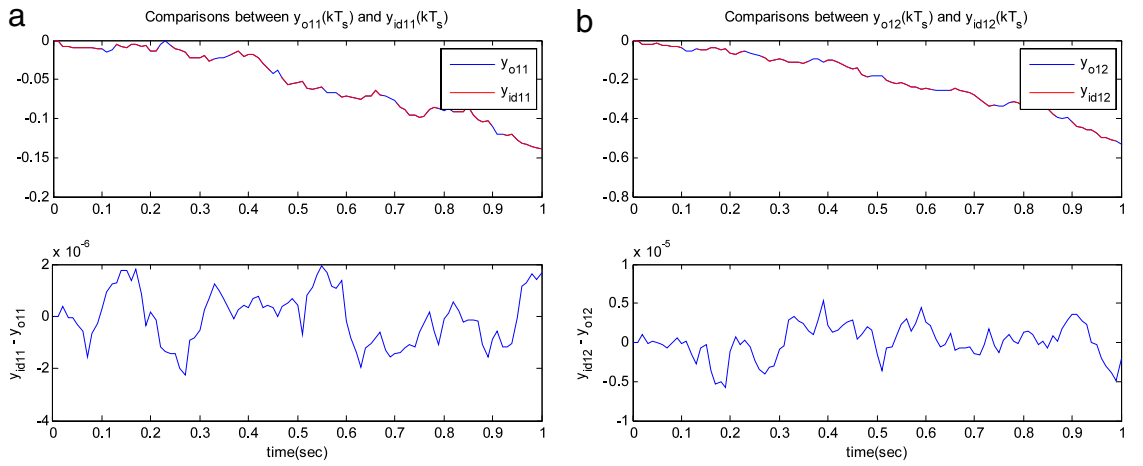

Fig. 7. (a) The comparison between Subsystem Σ_1 output $y_{id11}(kT_s)$ and its observer-based output $y_{o11}(kT_s)$ by digital redesign, (b) The comparison between Subsystem Σ_1 output $y_{id12}(kT_s)$ and its observer-based output $y_{o12}(kT_s)$ by digital redesign.

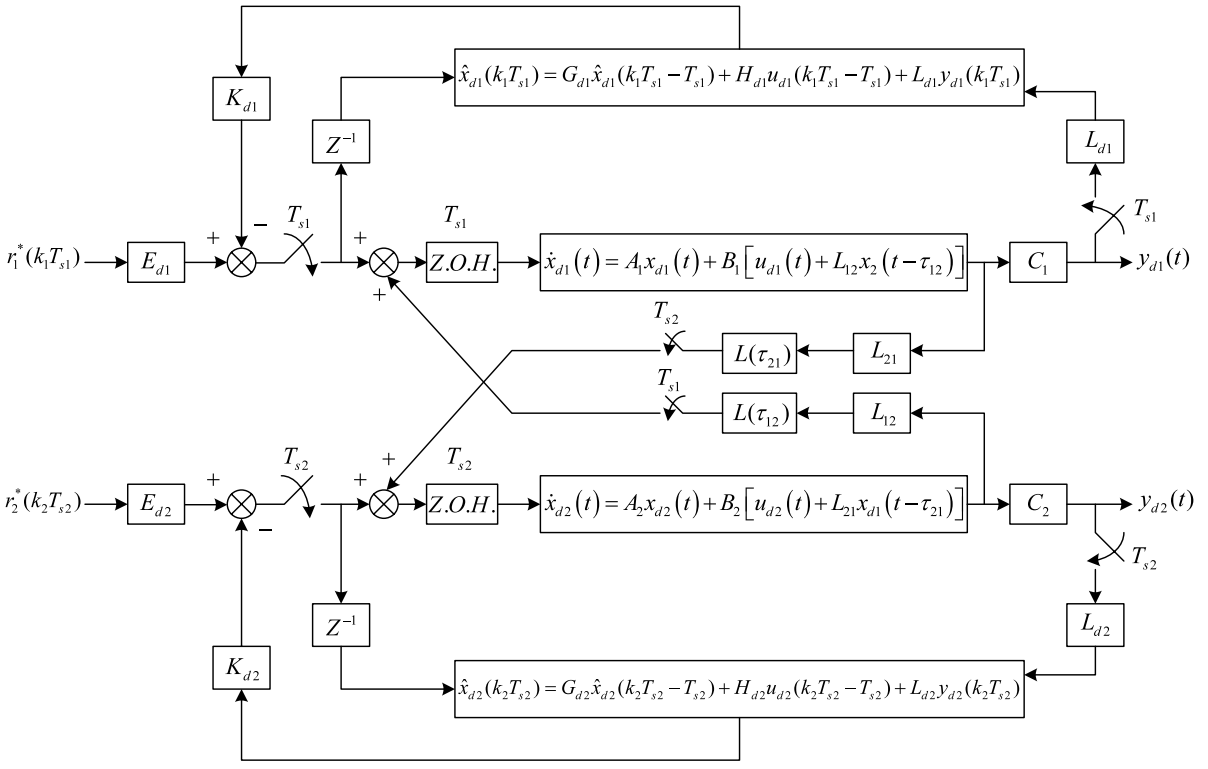

Fig. 8. The decentralized observer-based digital-redesigned tracker for the unknown linear sampled-data system with Type 1 interconnection.

The gain matrices of the observer-based digital tracker (65) for Subsystem Σ_1 and Subsystem Σ_2 are respectively given as

$$K_{d1} = 10^2 \times \begin{bmatrix} 0.4452 & -1.0093 & -0.4861 & -0.3476 \\ 2.2748 & -0.9496 & -1.5068 & -0.4948 \end{bmatrix}, \quad E_{d1} = 10^2 \times \begin{bmatrix} 1.0566 & -0.0239 \\ 2.089 & -1.0259 \end{bmatrix},$$

$$K_{d2} = 10^2 \times \begin{bmatrix} -0.3847 & 0.5729 & 0.3057 & -0.1043 \\ -0.1130 & -0.4530 & -0.0745 & 0.1947 \end{bmatrix}, \quad E_{d2} = 10^2 \times \begin{bmatrix} 0.4823 & -0.0541 \\ -0.2438 & -0.2199 \end{bmatrix},$$

with $Q_1 = 10^{10} \times I_2, R_1 = I_2, Q_2 = 10^{10} \times I_2, R_2 = I_2$. The reference input is given by $r(t) = \begin{bmatrix} \cos(10t) \\ \cos(10t) \end{bmatrix}$, and the output responses of the large-scale system for Subsystem Σ_1 and Subsystem Σ_2 are shown in Fig. 9. Here, we only show one of output responses and the other is similar.

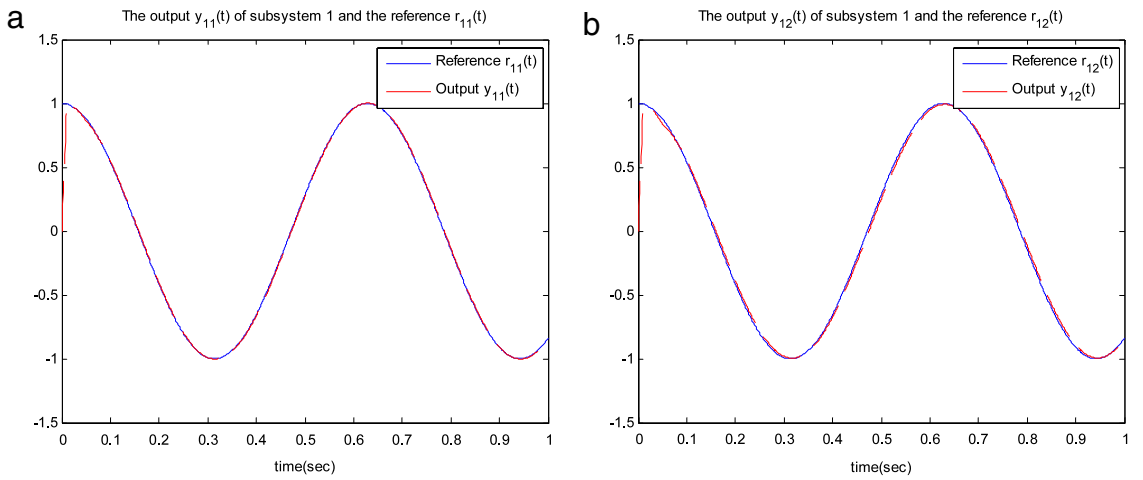

Fig. 9. (a) Output responses of Type 1 Subsystem Σ_1: output $y_{11}(t)$ and reference $r_{11}(t)$, (b) Output responses of Type 1 Subsystem Σ_2: output $y_{12}(t)$ and reference $r_{12}(t)$.

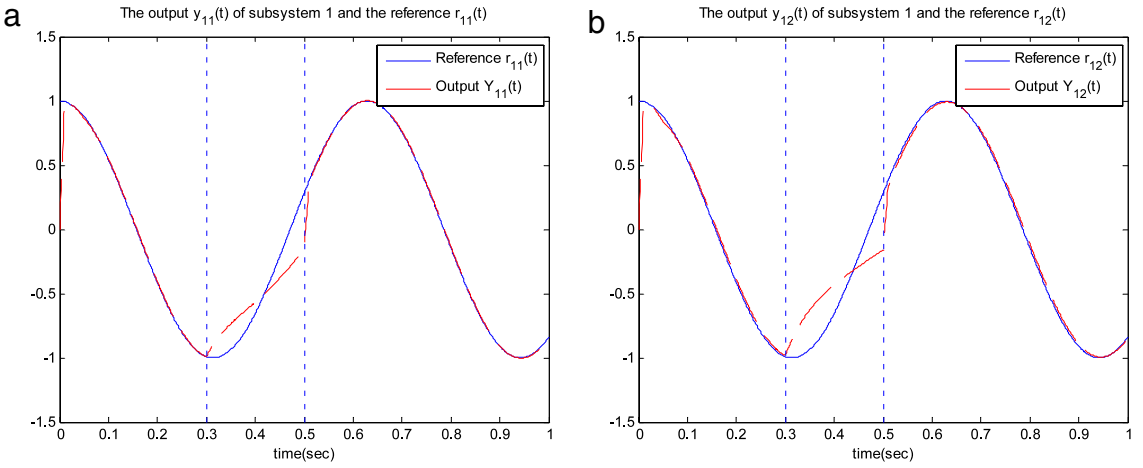

Fig. 10. (a) Output responses of Type 1 Subsystem Σ_1: output $y_{11}(t)$ and reference $r_{11}(t)$, (b) Output responses of Type 1 Subsystem Σ_2: output $y_{12}(t)$ and reference $r_{12}(t)$; The unanticipated failure occurs without fault-tolerant control during $t = 0.3$–0.5 s.

In order to confirm the independence of the control for the two subsystem, the control input $u_d(kT_s)$ of Subsystem Σ_1 is reduced by multiplying a scalar 0.1 during 0.3 s to 0.5 s in this simulation. Although the control input $u_d(kT_s)$ of Subsystem Σ_1 is reduced, the tracking performance of Subsystem Σ_2 will not be affected by this condition and the results are shown in Figs. 10 and 11.

6.2. A MIMO large-scale unknown nonlinear system

Consider the large-scale unknown system that contains two interconnected two-in-two-out subsystems described as follows:

$$\Sigma_1 : \dot{x}_1(t) = f_1(x_1(t)) + g_1(x_1(t))\,[u_1(t) + h_{12}(x_2(t - \tau_{12}))]; \qquad y_1(t) = C_1 x_1(t), \tag{68}$$

$$\Sigma_2 : \dot{x}_2(t) = f_2(x_2(t)) + g_2(x_2(t))\,[u_2(t) + h_{21}(x_1(t - \tau_{21}))]; \qquad y_2(t) = C_2 x_2(t), \tag{69}$$

where $u_1(t) = \begin{bmatrix} u_{1,1}(t) \\ u_{1,2}(t) \end{bmatrix}$, $u_2(t) = \begin{bmatrix} u_{2,1}(t) \\ u_{2,2}(t) \end{bmatrix}$, $x_1(t) = \begin{bmatrix} x_{1,1}(t) & x_{1,2}(t) & x_{1,3}(t) & x_{1,4}(t) \end{bmatrix}^T$, $x_2(t) = [x_{2,1}(t)\ x_{2,2}(t)\ x_{2,3}(t)\ x_{2,4}(t)]^T$.

The first Subsystem Σ_1 of the large-scale system is given by two-link robot (Fig. 12), which is described as follows:

The dynamic equation of the two-link robot system can be expressed as follows:

$$M(q)\ddot{q} + C(q, \dot{q})\dot{q} + G(q) = \Gamma, \tag{70}$$

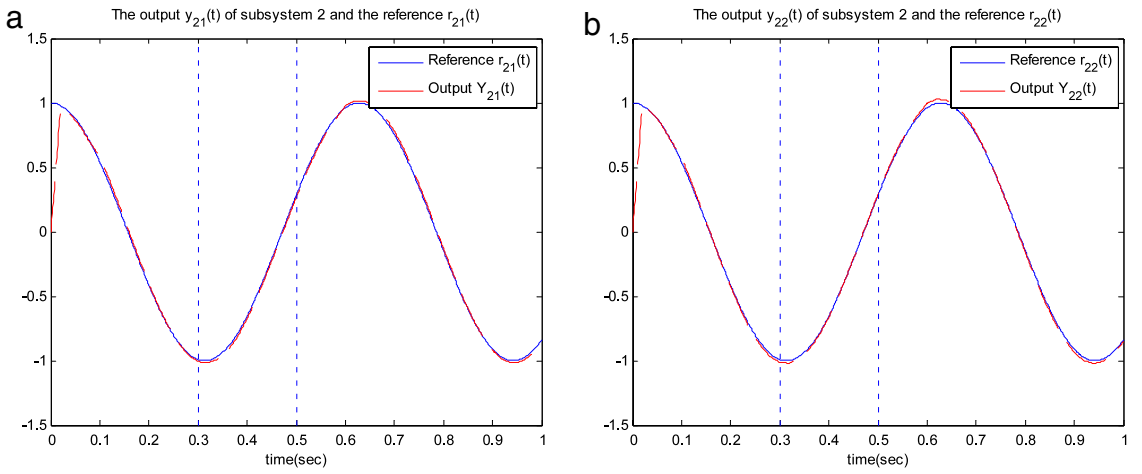

Fig. 11. (a) Output responses of Type 1 Subsystem Σ_1: output $y_{21}(t)$ and reference $r_{21}(t)$, (b) Output responses of Type 1 Subsystem Σ_2: output $y_{22}(t)$ and reference $r_{22}(t)$; The unanticipated failure occurs without fault-tolerant control during $t = 0.3$–0.5 s.

where

$$M(q) = \begin{bmatrix} (m_1+m_2)l_1^2 & m_2 l_1 l_2 (s_1 s_2 + c_1 c_2) \\ m_2 l_1 l_2 (s_1 s_2 + c_1 c_2) & m_2 l_2^2 \end{bmatrix}, \qquad C(q,\dot{q}) = m_2 l_1 l_2 (c_1 s_2 - s_1 c_2) \begin{bmatrix} 0 & -\dot{q}_2 \\ -\dot{q}_1 & 0 \end{bmatrix},$$

$G(q) = \begin{bmatrix} -(m_1+m_2) l_1 g_r s_1 \\ -m_2 l_2 g_r s_2 \end{bmatrix}$, and $q = \begin{bmatrix} q_1 & q_2 \end{bmatrix}^T$, q_1, q_2 are the angular positions, $M(q)$ is the moment of inertia, $C(q,\dot{q})$ includes coriolis and centripetal forces, $G(q)$ is the gravitational force, Γ is the applied torque vector. Here, we use the short hand notations $s_i = \sin(q_i)$ and $c_i = \cos(q_i)$. The nominal parameters of the system are given as the link masses $m_1 = 5$ kg, $m_2 = 2.5$ kg, the length $l_1 = l_2 = 0.5$ m, and the gravitational acceleration $g_r = 9.81$ ms^{-2}. Rewrite (71) in the following form

$$\ddot{q} = M^{-1}(q)(\Gamma - C(q,\dot{q})\dot{q} - G(q)). \tag{71}$$

Let x_1 and $f_1(x_1)$ present the state of the system and the nonlinear function of the state x_1 respectively. And the notation is shown as

$$x_1(t) \triangleq [x_{1,1} \quad x_{1,2} \quad x_{1,3} \quad x_{1,4}]^T = [q_1 \quad \dot{q}_1 \quad q_2 \quad \dot{q}_2]^T, \qquad f_1(x_1(t)) \triangleq [f_{1,1} \quad f_{1,2} \quad f_{1,3} \quad f_{1,4}]^T,$$

where $f_{1,1} = x_{1,2}, f_{1,3} = x_{1,4}, [f_{1,2} \quad f_{1,4}]^T = M^{-1}(-C[x_{1,2} \quad x_{1,4}]^T - G)$, Also let $u_1 \triangleq \Gamma$, where $\Gamma = \begin{bmatrix} \Gamma_1 & \Gamma_2 \end{bmatrix}^T$. Calculate the inverse of the matrix M, then one has $M^{-1} = \begin{bmatrix} p_{11} & p_{12} \\ p_{21} & p_{22} \end{bmatrix}$ such that $g_1(x_1(t)) = \begin{bmatrix} 0 & p_{11} & 0 & p_{21} \\ 0 & p_{12} & 0 & p_{22} \end{bmatrix}^T$. So the dynamic equation of the two-link robot system can be reformulated as follows

$$\dot{x}_1(t) = f_1(x_1(t)) + g_1(x_1(t)) u_1(t), \tag{72a}$$
$$y_1 = C_1 x_1, \tag{72b}$$

where $C_1 = \begin{bmatrix} 1 & 0 & 0 & 0 \\ 0 & 0 & 1 & 0 \end{bmatrix}$ and the initial condition $x_1(0) = \begin{bmatrix} 0 & 0 & 0 & 0 \end{bmatrix}^T$. The second Subsystem Σ_2 of the large-scale system is given by mass-spring-damper system, which is described as follows:

The dynamic equation of the mass-spring-damper system (Fig. 13) can be expressed as follows:

$$(M_1 + \Delta M_1)\ddot{y}_1 = f_{u1} - f_{K1}(x) - f_{B1}(x) + f_{K2}(x) + f_{B2}(x) - f_{C1}(x) + f_{C2}(x) + d_1, \tag{73}$$
$$(M_2 + \Delta M_2)\ddot{y}_2 = f_{u2} - f_{K2}(x) - f_{B2}(x) - f_{C2}(x) + d_2, \tag{74}$$

where $x \triangleq \begin{bmatrix} y_1 & \dot{y}_1 & y_2 & \dot{y}_2 \end{bmatrix}^T$, the spring forces $f_{K1}(x) = K_{10} y_1 + \Delta K_1 y_1^3$, $f_{K2}(x) = K_{20}(y_2 - y_1) + \Delta K_2 (y_2 - y_1)^3$, the friction forces $f_{B1}(x) = B_{10}\dot{y}_1 + \Delta B_1 \dot{y}_1^2$, $f_{B2}(x) = B_{20}(\dot{y}_2 - \dot{y}_1) + \Delta B_2 (\dot{y}_2 - \dot{y}_1)^2$ and the coulomb friction forces $f_{C1} = 0.02 sgn(\dot{y}_1)$, $f_{C2} = 0.02 sgn(\dot{y}_2 - \dot{y}_1)$. The nominal parameters are given as $M_1 = 0.25$, $M_2 = 0.2$, $K_1 = 1$, $K_2 = 2$ and $B_1 = 2.2$. The perturbations are given as $\Delta M_1 = 0.05 \sin(y_1)$, $\Delta M_2 = 0.05 \sin(y_1 - y_2)$, $\Delta K_1 = 0.1$, $\Delta K_2 = 0.12$, $\Delta B_1 = 0.2$, $\Delta B_2 = 0.15$, $d_1 = 0.2 \sin(3t) \exp(-0.2t)$ and $d_2 = 0.2 \cos(3t) \exp(-0.1t)$.

Let x_2 and $f_2(x_2)$ present the state of the system and the nonlinear function of the state x_2 respectively. And the notation is shown as

$$x_2(t) \triangleq [x_{2,1} \quad x_{2,2} \quad x_{2,3} \quad x_{2,4}]^T = [y_1 \quad \dot{y}_1 \quad y_2 \quad \dot{y}_2]^T, \qquad f_2(x_2(t)) \triangleq [f_{2,1} \quad f_{2,2} \quad f_{2,3} \quad f_{2,4}]^T,$$

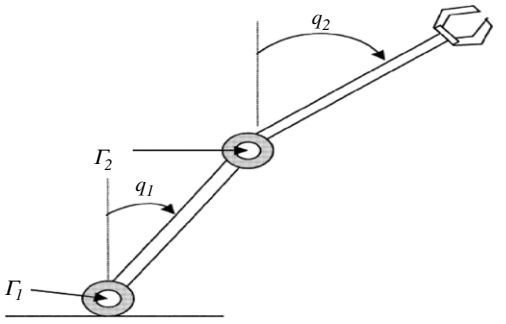

Fig. 12. Two-link robot.

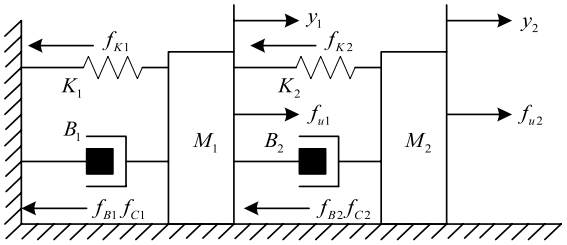

Fig. 13. Mass-spring-damper system.

where

$$f_{2,1} = x_{2,2}, \qquad f_{2,2} = \frac{1}{(M_1 + \Delta M_1)}(-f_{K1}(x_2) - f_{B1}(x_2) + f_{K2}(x_2) + f_{B2}(x_2) - f_{C1}(x_2) + f_{C2}(x_2) + d_1),$$
$$f_{2,3} = x_{2,4}, \qquad f_{2,4} = \frac{1}{(M_2 + \Delta M_2)}(-f_{K2}(x_2) - f_{B2}(x_2) - f_{C2}(x_2) + d_2),$$

and $g_2(x_2(t)) = \begin{bmatrix} 0 & \frac{1}{(M_1+\Delta M_1)} & 0 & 0 \\ 0 & 0 & \frac{1}{(M_2+\Delta M_2)} & 0 \end{bmatrix}^T$. Also, let $u_2 \triangleq f_u$, where $f_u = \begin{bmatrix} f_{u1} & f_{u2} \end{bmatrix}^T$.

So the dynamic equation of the mass-spring-damper system can be reformulated as follows

$$\dot{x}_2(t) = f_2(x_2(t)) + g_2(x_2(t))u_2(t), \tag{75a}$$
$$y_2 = C_2 x_2, \tag{75b}$$

where $C_2 = \begin{bmatrix} 1 & 0 & 0 & 0 \\ 0 & 0 & 1 & 0 \end{bmatrix}$ and the initial condition $x_2(0) = \begin{bmatrix} 0.5 & 0 & 0 & 0 \end{bmatrix}^T$.

Combining the above systems with the nonlinear interconnected terms, the large-scale system can then be shown in Fig. 4a, where the nonlinear inter-connected terms $h_{12}(x_{d2}(t))$ and $h_{21}(x_{d1}(t))$ are given as $\begin{bmatrix} x_{d2,3}^2 \cos(x_{d2,1}) \\ \sin^2(x_{d2,2}) \end{bmatrix}$ and $\begin{bmatrix} x_{d1,1}^2 \\ x_{d1,3} \sin(x_{d1,2}) \end{bmatrix}$, respectively. The time delays of the nonlinear interconnected terms are $\tau_{21} = 2 \times T_{s1}$ and $\tau_{12} = 3 \times T_{s2}$, where $T_{s1} = 0.01$ s and $T_{s2} = 0.02$ s (see Figs. 4a and 4b).

Let the open-loop system be excited by the control force $u(t)$ with white noise $u(t) = \begin{bmatrix} u_1(t) & u_2(t) \end{bmatrix}^T$ having a zero mean and covariance $diag\,[cov(u_1(t)), cov(u_2(t))] = diag\,\begin{bmatrix} 0.2 & 0.2 \end{bmatrix}$, where the sampling times $T_{s1} = 0.01$ s and $T_{s2} = 0.02$ s for Subsystem Σ_1 and Subsystem Σ_2 respectively. We can get input–output sampled data in Fig. 14.

Similar to 1, the identified system and observer by OKID for Subsystem Σ_1 and Subsystem Σ_2 can be obtained. Then, the observer-based outputs compared with the actual system outputs for Subsystem Σ_1 are shown in Fig. 15, and Subsystem Σ_2 has similar simulation results.

To overcome the effect of modeling error, an improved observer with the high-gain property based on the digital-redesign approach has been used in (65). Then, the comparisons between the actual outputs and their observer-based outputs by digital redesign for Subsystem Σ_1 are shown in Fig. 16, and certainly the results for Subsystem Σ_2 are similar to Σ_1.

The gain matrices of observer-based digital tracker (65) for Subsystem Σ_1 and Subsystem Σ_2 are respectively given. For Type 1 and Type 2, the reference input is given by $r(t) = \begin{bmatrix} 0.5\sin(t) \\ 0.5\cos(t) \end{bmatrix}$ and the output responses of the large-scale system for Subsystem Σ_1 are shown in Figs. 17 and 18, respectively. Here, we omit the results of Subsystem Σ_2.

In order to confirm the independence of the control for the two subsystems, the control input $u_d(kT_s)$ of Subsystem Σ_1 is reduced by multiplying a scalar 0.02 during 2 s to 4 s in this simulation. Although the control input $u_d(kT_s)$ of Subsystem Σ_1 is reduced, the tracking performance of Subsystem Σ_2 will not be affected by this condition and the results are shown in Figs. 19–22.

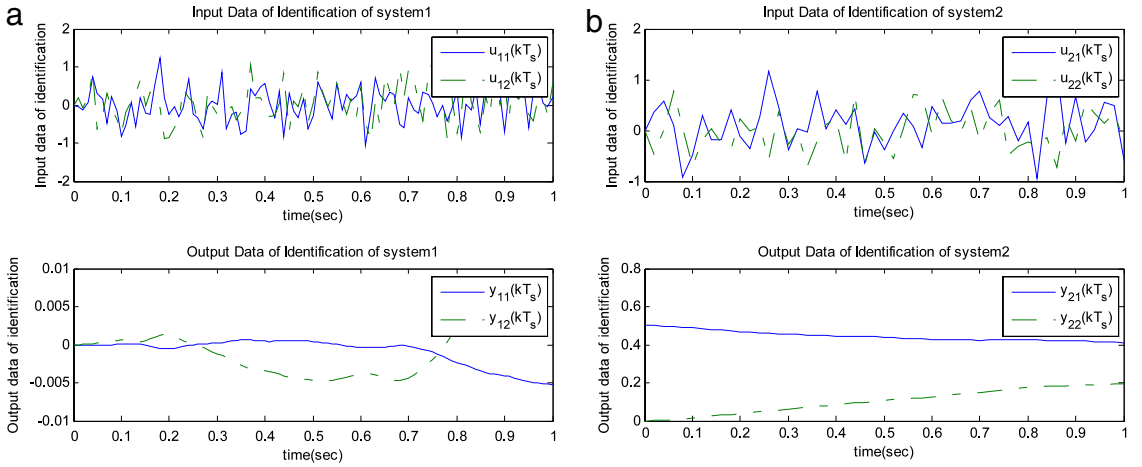

Fig. 14. (a) Subsystem Σ_1 I/O data for identification, (b) Subsystem Σ_2 I/O data for identification.

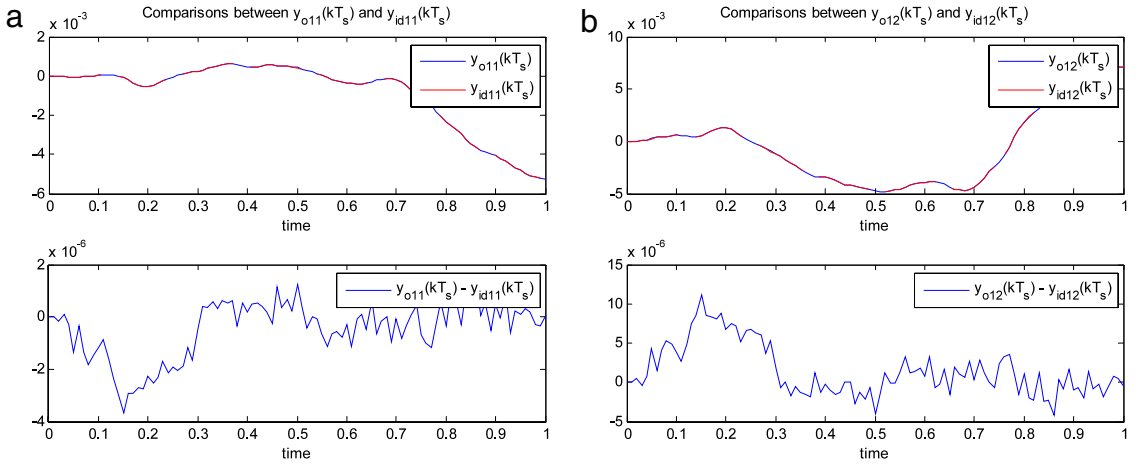

Fig. 15. (a) The comparison between Subsystem Σ_1 output $y_{id11}(kT_s)$ and its observer-based output $y_{o11}(kT_s)$ by OKID, (b) The comparison between Subsystem Σ_1 output $y_{id12}(kT_s)$ and its observer-based output $y_{o12}(kT_s)$ by OKID.

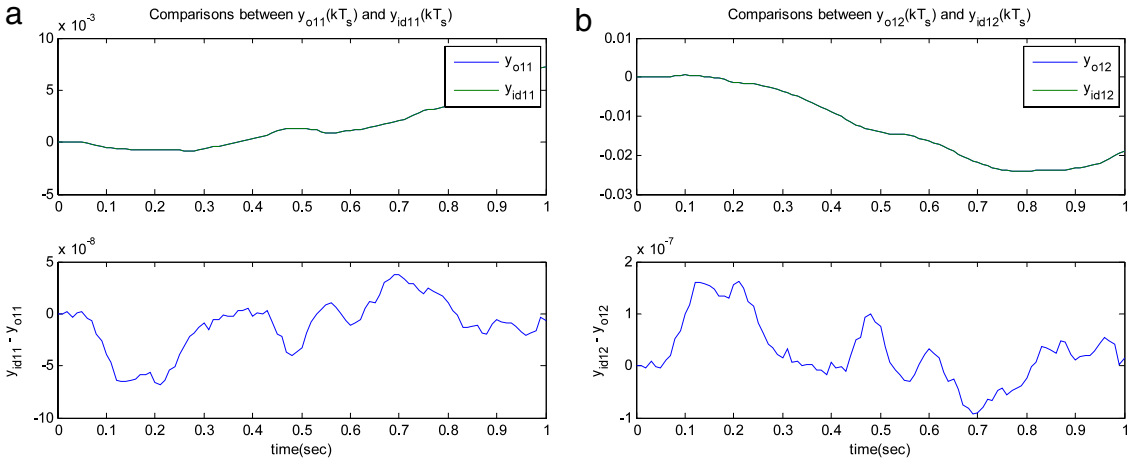

Fig. 16. (a) The comparison between Subsystem Σ_1 output $y_{id11}(kT_s)$ and its observer-based output $y_{o11}(kT_s)$ by digital redesign, (b) The comparison between Subsystem Σ_1 output $y_{id12}(kT_s)$ and its observer-based output $y_{o12}(kT_s)$ by digital redesign.

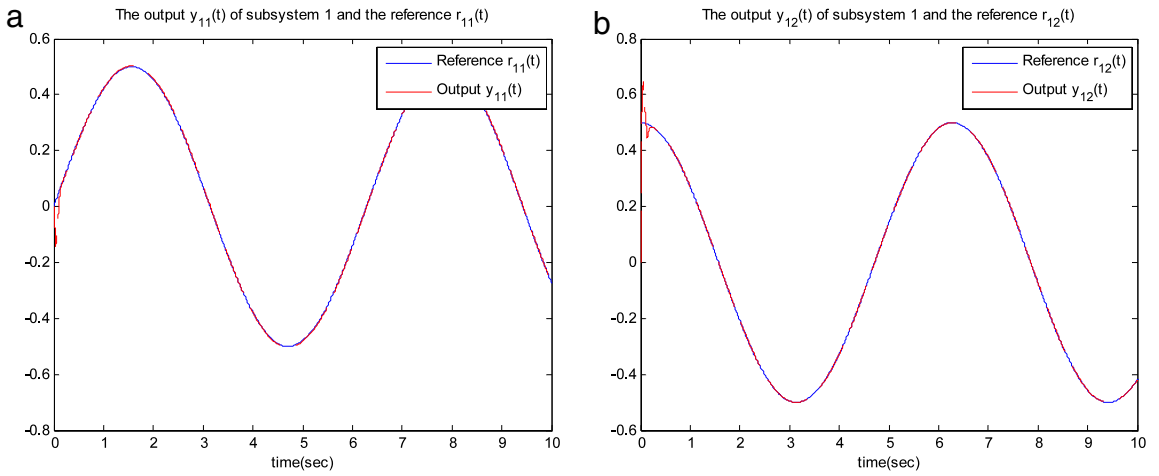

Fig. 17. (a) Output responses of Type 1 Subsystem Σ_1: output $y_{11}(t)$ and reference $r_{11}(t)$, (b) Output responses of Type 1 Subsystem Σ_1: output $y_{12}(t)$ and reference $r_{12}(t)$.

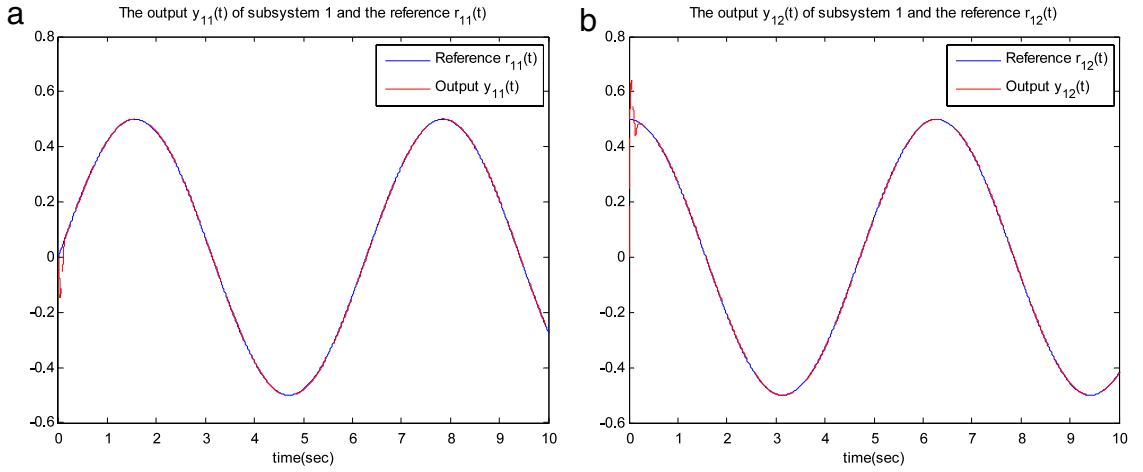

Fig. 18. (a) Output responses of Type 2 Subsystem Σ_1: output $y_{11}(t)$ and reference $r_{11}(t)$, (b) Output responses of Type 2 Subsystem Σ_1: output $y_{12}(t)$ and reference $r_{12}(t)$.

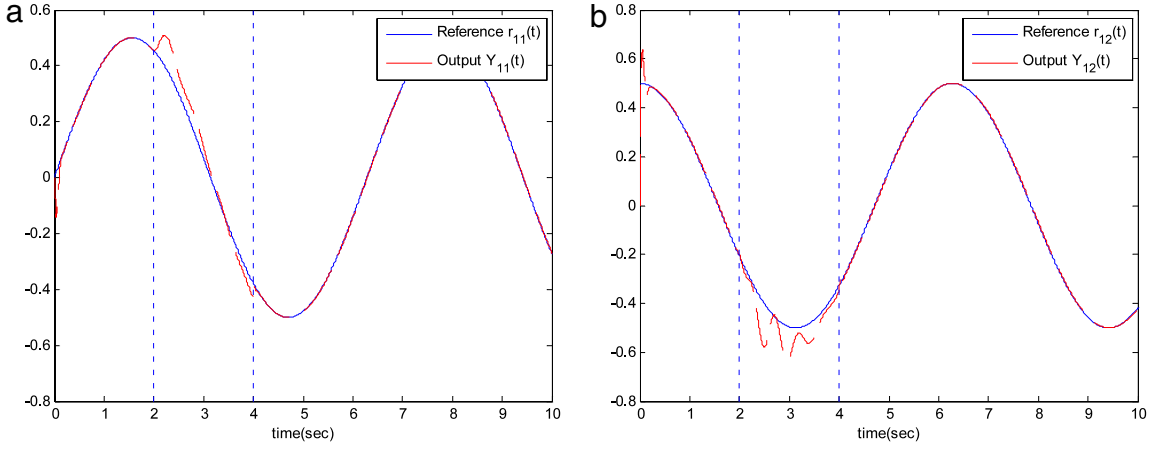

Fig. 19. (a) Output responses of Type 1 Subsystem Σ_1: output $y_{11}(t)$ and reference $r_{11}(t)$, (b) Output responses of Type 1 Subsystem Σ_1: output $y_{12}(t)$ and reference $r_{12}(t)$; The unanticipated failure occurs without fault-tolerant control during $t = 2$–4 s.

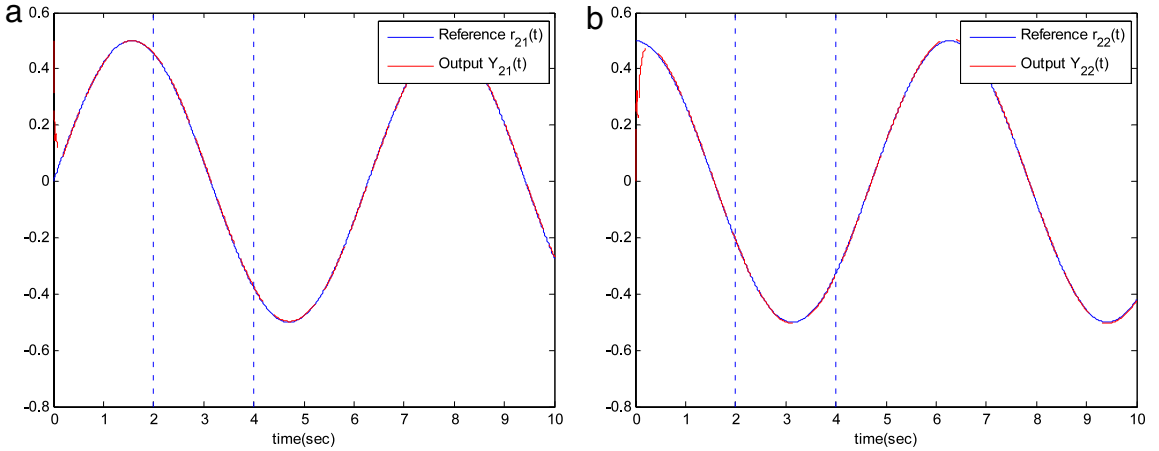

Fig. 20. (a) Output responses of Type 1 Subsystem Σ_2: output $y_{21}(t)$ and reference $r_{21}(t)$, (b) Output responses of Type 1 Subsystem Σ_2: output $y_{22}(t)$ and reference $r_{22}(t)$; The unanticipated failure occurs without fault-tolerant control during $t = 2$–4 s.

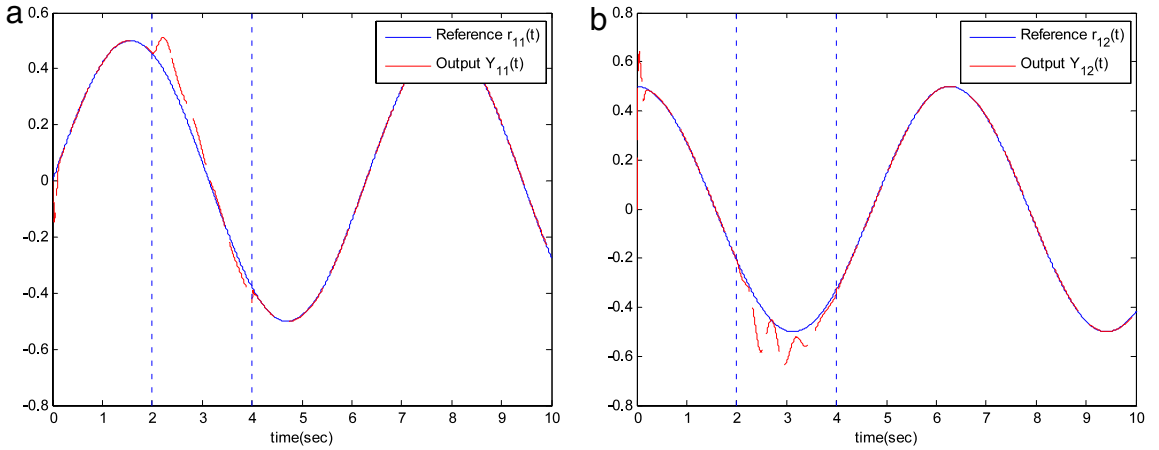

Fig. 21. (a) Output responses of Type 2 Subsystem Σ_1: output $y_{11}(t)$ and reference $r_{11}(t)$, (b) Output responses of Type 2 Subsystem Σ_1: output $y_{12}(t)$ and reference $r_{12}(t)$; The unanticipated failure occurs without fault-tolerant control during $t = 2$–4 s.

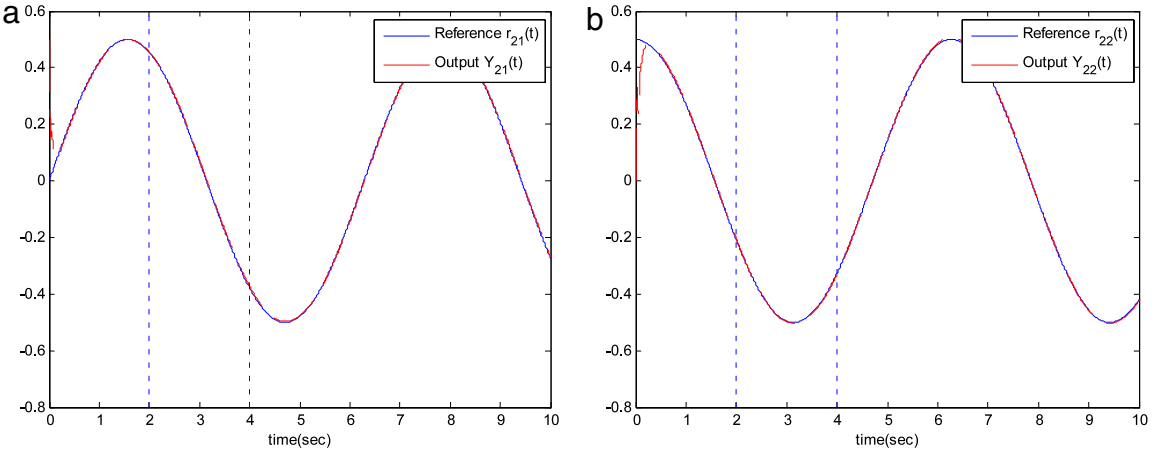

Fig. 22. (a) Output responses of Type 2 Subsystem Σ_2: output $y_{21}(t)$ and reference $r_{21}(t)$, (b) Output responses of Type 2 Subsystem Σ_2: output $y_{22}(t)$ and reference $r_{22}(t)$; The unanticipated failure occurs without fault-tolerant control during $t = 2$–4 s.

7. Conclusion

A connection between the appropriate (low-)order decentralized linear observer and some class of unknown interconnected large-scale sampled-data nonlinear system has been constructed via the observer/Kalman filter identification method. The OKID method is a time-domain technique that identifies a discrete input–output mapping by using known input–output sampled data in the general coordinate form, though an extension of the eigensystem realization algorithm (ERA). Therefore, the appropriate (low) orders of the decentralized observer can be determined. To overcome the effect of modeling error, an improved observer with the high-gain property based on the digital-redesign approach has been proposed in this paper. Consequently, the digital-redesign-based decentralized tracker with the high-gain property yields the high performance tracking purpose and the closed-loop system has the property of decoupling, such that when some unanticipated fault occurs in some subsystem will not affect the tracking performance of other subsystem. The proposed approach is significantly useful for the class of large-scale sampled-data nonlinear systems with known or unknown system equation.

Acknowledgements

This work was supported by the National Science Council of Republic of China under contracts NSC96-2221-E-006-292-MY3 and NSC98-2221-E-006-159-MY3, the US Army Research Office under grant W911NF-06-1-0507, the National Science Foundation under grant NSF 0717860, and the research contract 1440234.

References

[1] H.S. Wu, Decentralized robust control for a class of large-scale interconnected systems with uncertainties, Internat. J. Systems Sci. 20 (12) (1989) 2597–2608.
[2] M. Jamshidi, Largescale System: Modeling and Control, Elserier Science Publishing, New York, 1983.
[3] E.J. Davison, The robust decentralized control of servomechanism problem for composite system with input–output interconnection, IEEE Trans. Automat. Control 24 (2) (1979) 325–327.
[4] P.A. Ioannou, J. Sun, Robust Adaptive Control, Prentice Hall, New Jersey, 1996.
[5] D.T. Gavel, D.D. Seljuk, Decentralized adaptive control: structural conditions for stability, IEEE Trans. Automat. Control 34 (1989) 413–426.
[6] L. Shi, S.K. Singh, Decentralized adaptive controller design of large-scale systems with higher order interconnections, IEEE Trans. Automat. Control 37 (1992) 1106–1118.
[7] R. Ortega, A. Herrera, A solution to the decentralized adaptive stabilization problem, Systems Control Lett. 20 (1993) 299–306.
[8] A. Datta, Performance improvement in decentralized adaptive control: a modified model reference scheme, IEEE Trans. Automat. Control 38 (11) (1993) 1717–1722.
[9] Y.H. Chen, G. Leitmann, Z.K. Xiong, Robust control design for interconnected systems with time-varying uncertainties, Internat. J. Control 54 (1991) 1119–1124.
[10] C. Wen, Direct decentralized adaptive control of interconnected systems having arbitrary subsystem relative degrees, in: Proc. of the Decision and Control Conference, Lake Buena Vista, FL, Dec. 14–16, 1994 pp. 1187–1192.
[11] C. Wen, Indirect robust totally decentralized adaptive control of continuous-time interconnected systems, IEEE Trans. Automat. Control 38 (6) (1995) 1122–1126.
[12] K. Ikeda, S. Shin, Fault tolerant decentralized control systems using backstepping, in: Proc. of the Decision and Control Conference, New Orleans, LA, Dec. 14–16, 1995 pp. 2340–2345.
[13] P.R. Pagilla, Robust decentralized control of large-scale interconnected systems: general interconnections, in: Proc. of the American Control Conference, San Diego, CA, June 2–4, 1999 pp. 4527–4531.
[14] O. Huseyin, M.E. Sezer, D.D. Siljak, Robust decentralized control using output feedback, IEE Proceedings 129 (1982) 310–314.
[15] A. Datta, P.A. Ioannou, Decentralized indirect adaptive control of interconnected systems, Internat. J. Adapt. Control. Signal Process. 5 (4) (1991) 259–281.
[16] K.S. Narendra, A.M. Annaswamy, Stable Adaptive Systems, Prentice-Hall, Upper Saddle River, New Jersey, 1989.
[17] K.S. Narendra, N.O. Oleng', Exact output tracking in decentralized adaptive control systems, Center for Systems Science, Yale University, New Haven, CT, Tech. Rep. 0104, 2001.
[18] J.N. Juang, Applied System Identification, Prentice-Hall, Englewood Cliffs, NJ, 1994.
[19] S.M. Guo, L.S. Shieh, G. Chen, C.F. Lin, Effective chaotic orbit tracker: a prediction-based digital redesign approach, IEEE Trans. Circuits Syst. I Fundam. Theory Appl. 47 (11) (2000) 1557–1570.
[20] H. Fujimoto, A. Kawamura, M. Tomizuka, Generalized digital redesign method for linear feedback system based on N-delay control, IEEE-ASME Trans. Mech. 4 (2) (1999) 101–109.
[21] W. Chang, J.B. Park, H.J. Lee, Y.H. Joo, LMI approach to digital redesign of linear time invariant systems, IEE Proc. Control Theory Appl. 149 (4) (2002) 297–302.
[22] H.J. Lee, J.B. Park, Y.H. Joo, Further refinement on LMI-based digital redesign: delta-operator approach, IEEE Trans. Circuits Syst. II Express Briefs 53 (6) (2006) 473–477.
[23] H.J. Lee, L.-S. Shieh, D.W. Kim, Digital control of nonlinear systems: optimal linearization-based digital redesign approach, IET Control Theory Appl. 2 (4) (2008) 337–351.
[24] H.J. Lee, J.B. Park, Y.H. Joo, An efficient observer-based sampled-data control: digital redesign approach, IEEE Trans. Circuits Syst. I Fundam. Theory Appl. 50 (12) (2003) 1595–1601.
[25] M. Phan, L.G. Horta, J.N. Juang, R.W. Longman, Linear system identification via an asymptotically stable observer, J. Optim. Theory Appl. 79 (1) (1993) 59–86.
[26] C. Kuo, Digital Control System, Holt, Rinehart and Winston, New York, 1980.